

BOEING

CODE IDENT. NO. 81205

NUMBER D2-100819-1

TITLE: DEVELOPMENT OF A SIMPLE LUNAR MODEL FOR APOLLO -
FINAL REPORT

**CASE FILE
COPY**

SEATTLE, WASHINGTON

DEVELOPMENT OF A SIMPLE LUNAR MODEL FOR APOLLO

By Ralph E. Risdal

Distribution of this report is provided in the interest of information exchange. Responsibility for the contents resides in the author or organization that prepared it.

Prepared under Contract No. NAS1-7954 by
THE BOEING COMPANY
Seattle, Washington

for

NATIONAL AERONAUTICS AND SPACE ADMINISTRATION

THE **BOEING** COMPANY

REV LTR

CODE IDENT. NO. 81205

NUMBER D2-100819-1

TITLE: DEVELOPMENT OF A SIMPLE LUNAR MODEL FOR APOLLO -
FINAL REPORT

ORIGINAL RELEASE DATE _____. FOR THE RELEASE DATE OF SUBSEQUENT REVISIONS, SEE THE REVISIONS SHEET. FOR LIMITATIONS IMPOSED ON THE DISTRIBUTION AND USE OF INFORMATION CONTAINED IN THIS DOCUMENT, SEE THE LIMITATIONS SHEET.

MODEL _____ CONTRACT NAS 1-7954

ISSUE NO. _____ ISSUED TO: _____

PREPARED BY R. E. Risdal
R. E. Risdal
SUPERVISED BY W. R. Burr
W. R. Burr
APPROVED BY L. B. Eldrenkamp 12/20/68
L. B. Eldrenkamp
APPROVED BY J. C. Graves 12/20/68
J. C. Graves

4/24/69

ABSTRACT

A simplified four coefficient lunar gravitational potential model has been developed for Apollo mission control. This model was developed using Lunar Orbiter tracking data. It provides accurate predictions of orbit element histories over a range of orbit inclinations and orbit eccentricities.

KEY WORDS

Lunar Model

Gravitational Potential

Lunar Orbiter

Apollo

Orbit Elements

USE FOR TYPEWRITTEN MATERIAL ONLY

TABLE OF CONTENTS

<u>SECTION</u>		<u>PAGE</u>
1.0	PURPOSE	1
2.0	SCOPE	2
3.0	INTRODUCTION	3
4.0	PROCEDURE	4
5.0	EFFECT OF GRAVITATIONAL MODEL COEFFICIENTS ON ORBIT ELEMENTS	5
6.0	CHARACTERISTICS OF SIMPLE LUNAR MODELS	19
6.1	Preliminary R-1 Model	19
6.2	R-2 Model	19
7.0	APOLLO ORBIT PERTURBATIONS	47
8.0	CONCLUSIONS AND RECOMMENDATIONS	52
9.0	REFERENCES	53
APPENDIX - ORBIT PERTURBATION EQUATIONS		54
<u>TABLES</u>		
5-1	Initial Conditions, Apollo Type Orbit	7
5-2	Effect of Coefficient	8
6-1	Initial Conditions	22
<u>FIGURES</u>		
5-1	Effect of J_{20} on Node Longitude	9
5-2	Effect of J_{20} on Argument of Perilune	10
5-3	Effect of J_{30} on Perilune Altitude	11
5-4	Effect of J_{30} on Orbit Inclination	12
5-5	Effect of J_{40} on Perilune Altitude	13
5-6	Effect of J_{40} on Node Longitude	14
5-7	Effect of J_{40} on Argument of Perilune	15
5-8	Effect of C_{22} on Orbit Inclination	16
5-9	Effect of C_{31} on Perilune Altitude	17
5-10	Effect of C_{31} on Argument of Perilune	18

USE FOR TYPEWRITTEN MATERIAL ONLY

TABLE OF CONTENTS (Continued)

<u>FIGURES</u>		<u>PAGE</u>
6-1	Perilune Altitude History, LO III-Phase 9 (R-1 Model)	23
6-2	Node Longitude History, LO III-Phase 9 (R-1 Model)	24
6-3	Argument of Perilune History, LO III-Phase 9 (R-1 Model)	25
6-4	Orbit Inclination History, LO III-Phase 9 (R-1 Model)	26
6-5	Perilune Altitude History, LO III-Phase 9 (R-2 Model)	27
6-6	Node Longitude History, LO III-Phase 9 (R-2 Model)	28
6-7	Argument of Perilune History, LO III-Phase 9 (R-2 Model)	29
6-8	Orbit Inclination History, LO III-Phase 9 (R-2 Model)	30
6-9		31
thru	Orbit Element History, LO III-Phase 6 (R-2 Model)	thru
6-12		34
6-13		35
thru	Orbit Element Histories, LO III-Phase 5 (R-2 Model)	thru
6-16		38
6-17		39
thru	Orbit Element Histories, LO I-Phase 7 (R-2 Model)	thru
6-20		42
6-21		43
thru	Orbit Element Histories, LO V-Phase 8 (R-2 Model)	thru
6-24		46
7-1	Perilune Altitude Prediction, Apollo Mission	48
7-2	Node Longitude Prediction, Apollo Mission	49
7-3	Argument of Perilune Prediction, Apollo Mission	50
7-4	Orbit Inclination Prediction, Apollo Mission	51

USE FOR TYPEWRITTEN MATERIAL ONLY

1.0 PURPOSE

This document reports the work accomplished under Task E of NASA contract NAS 1-7954 concerning lunar gravitational model analysis in support of Apollo mission control.

USE FOR TYPEWRITTEN MATERIAL ONLY

2.0 SCOPE

This document is a final report covering the work done under NASA contract NAS 1-7954, Task E. A simple four coefficient lunar gravitational model has been developed for application to Apollo mission control.

USE FOR TYPEWRITTEN MATERIAL ONLY

3.0 INTRODUCTION

Many studies have been initiated in an attempt to define an accurate lunar gravitational model based on tracking data obtained during the Lunar Orbiter program. Simple four coefficient models were developed during the program and were used successfully in mission control. Many high order models have been developed during and subsequent to the program. One of these high order models is presented in Reference 1. At the time the subject study was initiated, no one model had been developed which would accurately predict orbit element histories for the range of conditions encountered during the Lunar Orbiter program. Generally, the models were also very complicated, including up to sixty coefficients (seventh order).

The subject study was initiated in the attempt to develop a simple lunar model which would be applicable for Apollo mission control. Specifically, a model of approximately four coefficients or less was desired which would be significantly better than the triaxial moon model. This document describes the procedures used and defines the resulting simple four coefficient model (R-2) which was developed. The ability of the R-2 model to predict orbit elements is illustrated for several different orbits from Lunar Orbiter Mission I, III, and V. In addition, predictions are made of orbit element variations for a typical Apollo orbit.

Comparison of the R-2 model with other candidate lunar gravitational models is presented in a companion document (Reference 2). This document covers work done under Task D of NAS 1-7954 and compares the following capabilities of nine lunar models:

- . orbit determination convergence
- . in-orbit prediction
- . state vector mapping

USE FOR TYPEWRITTEN MATERIAL ONLY

4.0 PROCEDURE

Lunar gravitational coefficients are selected which exhibit a significant influence on at least one of the orbit elements. The number of coefficients is kept to a minimum in the interest of obtaining a simple model; a side benefit is realized in that there are essentially no problems due to correlation between coefficients. Once the coefficients are selected, then values are adjusted by an iterative process to obtain the best possible fit with Orbit Determination (OD) solutions from Lunar Orbiter tracking data. Data from Phase 9 of Lunar Orbiter III (also called the Apollo-type orbit) are used to develop the model, initially. This model is then checked against data from an earlier phase of Lunar Orbiter III and from Lunar Orbiters I and V.

Orbit element histories are defined by a digital computing program which implements the perturbation equations defined in the Appendix. Third body (Earth) effects are included in these equations.

USE FOR TYPEWRITTEN MATERIAL ONLY

5.0 EFFECT OF GRAVITATIONAL MODEL COEFFICIENTS ON ORBIT ELEMENTS

Effects of the model coefficients J_{20} , J_{30} , J_{40} , C_{22} and C_{31} on orbit elements are presented in this section. The orbit elements considered are: perilune altitude, inertial node longitude, argument of perilune, and orbit inclination. (Since semi-major axis remains constant, the effects on apolune altitude are opposite those on perilune altitude.)

The initial conditions used are those defined by OD 9001-8 (Table 5-1), which are the initial conditions of phase 9 of Lunar Orbiter III (also known as the Apollo type orbit). The "Apollo-type" orbit was achieved during the extended phase of Lunar Orbiter III mission after the photographic objectives were obtained. This orbit closely simulated the Apollo orbit and was obtained primarily for the purpose of providing the MSFN with tracking experience. The comments of this section pertain specifically to this type of an orbit and may not necessarily apply to other orbits.

It is well known that the second order zonal harmonic coefficient, J_{20} , has a direct effect on node longitude and argument of perilune. This fact is shown graphically in Figures 5-1 and 5-2. J_{20} also has an indirect effect on other orbit elements where the perturbations in these elements are functions of node longitude and argument of perilune. However, these effects are small and are not shown here. It is evident from the data shown that a value of J_{20} can be selected to provide an excellent fit of node longitude. This same value of J_{20} gives a good prediction of the average rate of change in argument of perilune. However, it does not provide for the short period oscillations. This value of J_{20} (2.1×10^{-4}) is essentially the same as the "accepted" value used in the triaxial moon model.

The most significant effect of J_{30} is to perturb eccentricity, and hence perilune altitude as shown in Figure 5-3. With the proper value of J_{30} , a good fit of perilune altitude can be obtained for the first 22 days, but there are large errors beyond that. J_{30} has an insignificant effect on node longitude and argument of perilune, but does have some effect on orbit inclination, as shown in Figure 5-4.

The fourth order zonal harmonic coefficient J_{40} has some effect on perilune altitude, as indicated in Figure 5-5. It can be seen, however, that it is not possible to get a good fit of perilune altitude over the 40-day period using J_{30} and J_{40} . J_{40} also has a significant effect on node longitude and argument of perilune, as shown in Figure 5-6 and 5-7. Therefore, for any value of J_{40} selected, J_{20} must be adjusted to obtain the desired variation in node longitude and argument of perilune. J_{40} provides no help in predicting the short period oscillation in argument of perilune.

The tesseral harmonic coefficient, C_{22} , has essentially no effect on any orbit element except inclination. The perturbations in orbit inclination are shown in Figure 5-8. Because of the scatter in the OD data, it is not possible to define a value of C_{22} on the basis of these data alone. However, it appears that the value of 2.1×10^{-5} (which is essentially the value from the triaxial moon model) provides a reasonable variation. (It will be shown in Section 6 that this value is valid.)

USE FOR TYPEWRITTEN MATERIAL ONLY

5.0 EFFECT OF GRAVITATIONAL MODEL COEFFICIENTS ON ORBIT ELEMENTS (Continued)

The four coefficients discussed above (J_{20} , J_{30} , J_{40} , and C_{22}) were originally considered for the simple lunar model. With these coefficients alone, it is not possible to obtain a good fit of perilune altitude or argument of perilune over the range of data available. It may be argued that argument of perilune is not important when in a near circular orbit and a good fit of perilune altitude is obtained for the first 22 days. This period of time is surely more than adequate for Apollo where the orbit duration will not be more than a few days. However it must be remembered that this good fit is for a particular set of initial conditions, and it will not be true for all initial conditions. For example, if the initial conditions as given by OD 9009-8 (shown at 21.3 days in Figure 5-3) were used, it is seen that there would be large errors in perilune altitude immediately. Therefore, it is important to define a model which will exhibit the correct trends, regardless of initial conditions.

In order to obtain a satisfactory model, an additional coefficient is required. Actually J_{40} is eliminated since it demonstrates no significant advantage. Another coefficient is sought which has little effect on node longitude and orbit inclination, while having a significant effect on eccentricity (hence perilune altitude) and argument of perilune. The perturbations due to this coefficient must also be a function of selenographic node longitude. After inspection of a complete set of orbit perturbation equations (through order 4), the coefficient C_{31} is selected.

The effects of C_{31} on perilune altitude are advantageous, as shown in Figure 5-9. Now it is seen that a satisfactory combination of J_{30} and C_{31} , is selected to give a good fit of perilune altitude. Figure 5-10 shows that the same value of C_{31} will also provide a very good fit of argument of perilune data.

The significant effects of the coefficients are summarized in Table 5-2. The values of these coefficients are now adjusted through an iterative process to define the lunar models which are discussed in the following section.

USE FOR TYPEWRITTEN MATERIAL ONLY

TABLE 5-1

INITIAL CONDITIONS, APOLLO TYPE ORBIT

Lunar Orbiter III, Phase 9
OD 9001-8

Epoch	
Date	8-30-67
Time (hr, min) GMT	20:55
Apolune Altitude, Km	315.59
Perilune Altitude, Km	144.46
Orbit Inclination, Deg.	20.88
Node Longitude (Selenographic)	deg. 63.93
Argument of perilune, Deg.	354.31

USE FOR TYPEWRITTEN MATERIAL ONLY

TABLE 5-2

EFFECT OF COEFFICIENTS

COEFFICIENT	ORBIT ELEMENT AFFECTED			
	PERILUNE ALTITUDE	NODE LONGITUDE	ARGUMENT OF PERILUNE	INCLINATION
J_{20}		•	•	
J_{30}	•			
J_{40}		•	•	
C_{22}				•
C_{31}	•		•	

EFFECT OF J_{20} ON
NODE LONGITUDE

INITIAL CONDITIONS : OD 9001-8

O OD SOLUTIONS

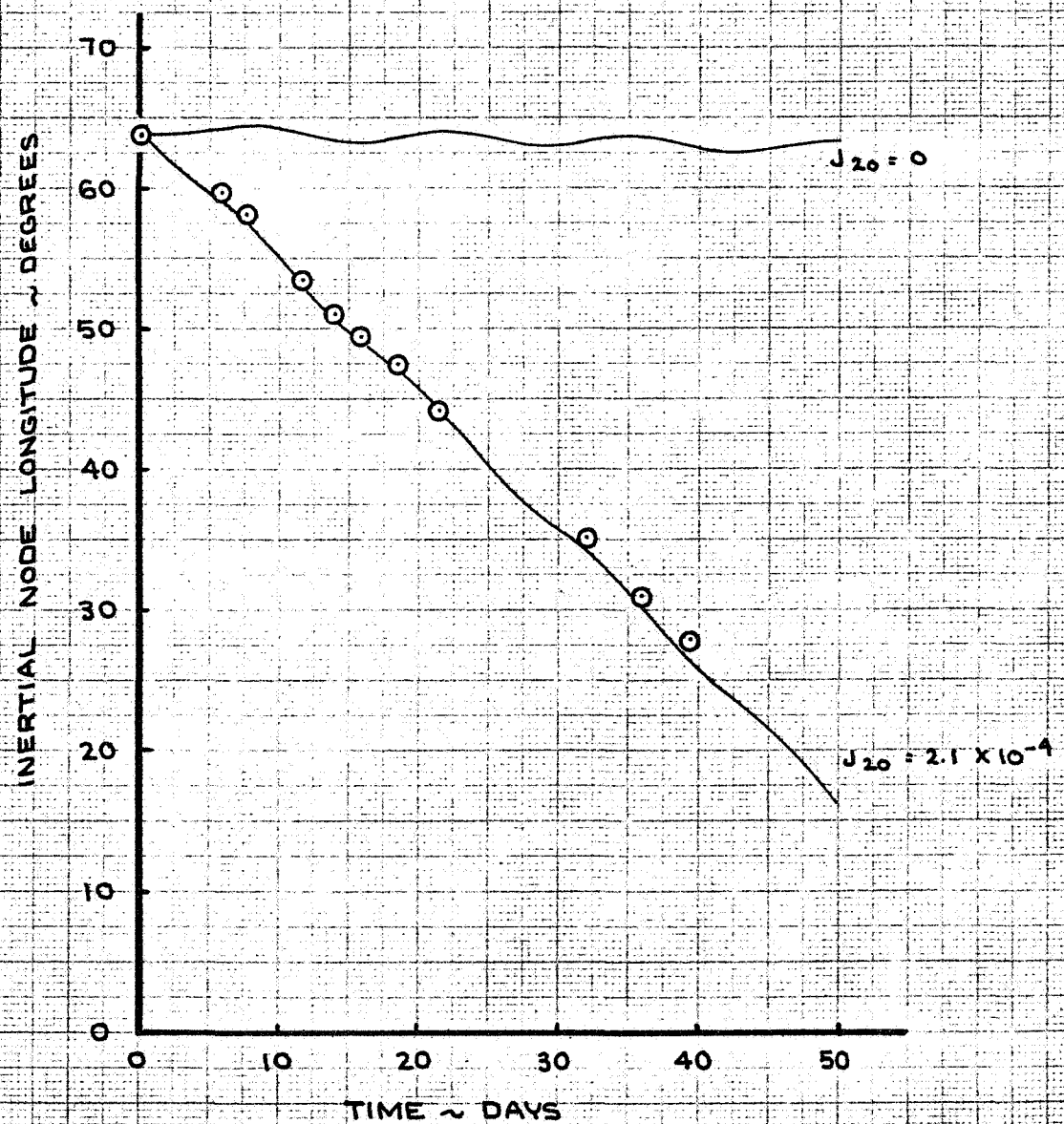
 $C_{22} = 2.1 \times 10^{-5}$ $J_{30} = -4.0 \times 10^{-5}$ 

FIGURE 5-1

EFFECT OF J_{20} ON
ARGUMENT OF PERILUNE

INITIAL CONDITIONS: OD 9001-8

O OD SOLUTIONS

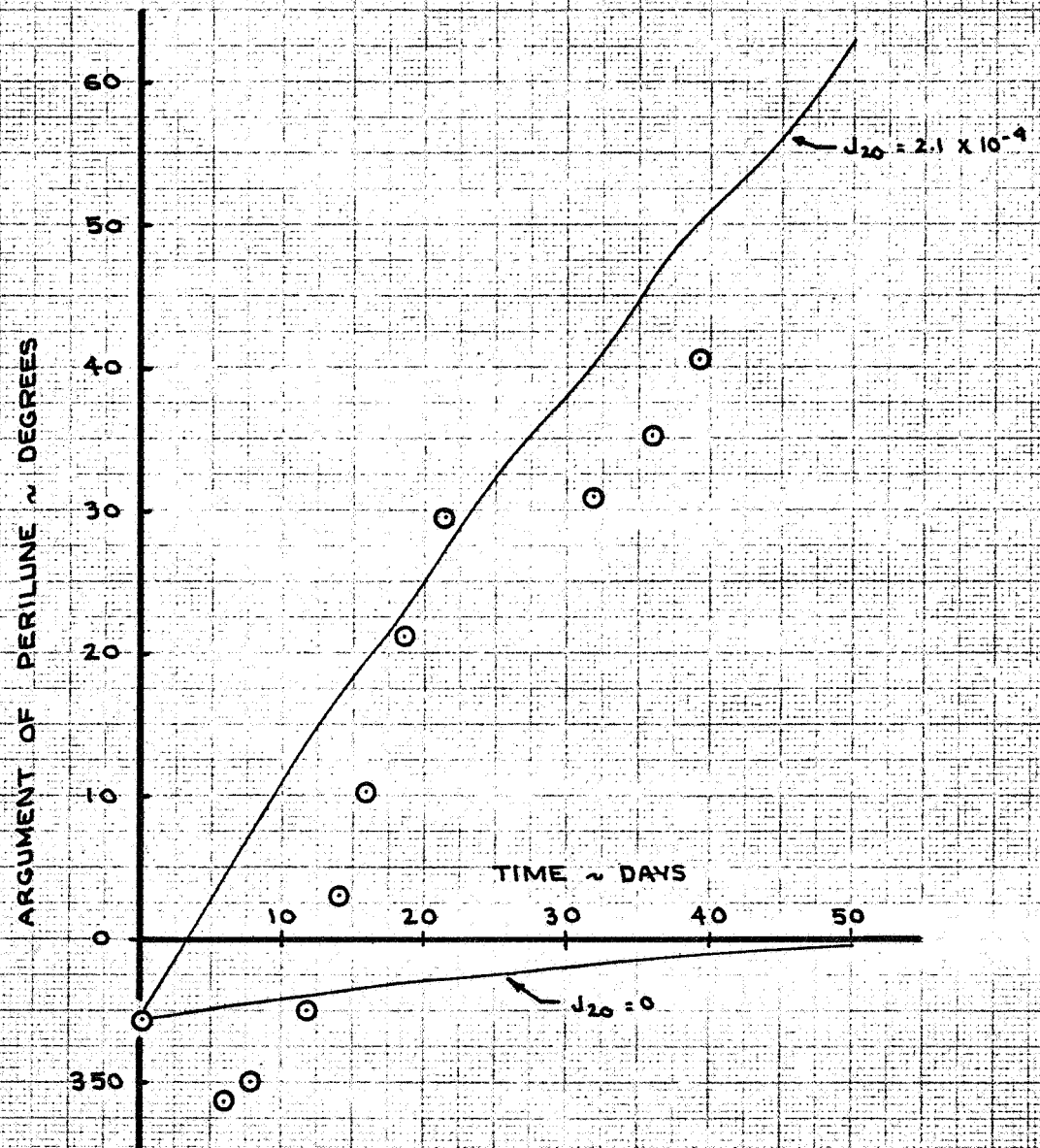
 $C_{22} = 2.1 \times 10^{-5}$ $J_{30} = -4.0 \times 10^{-5}$ 

FIGURE 5-2

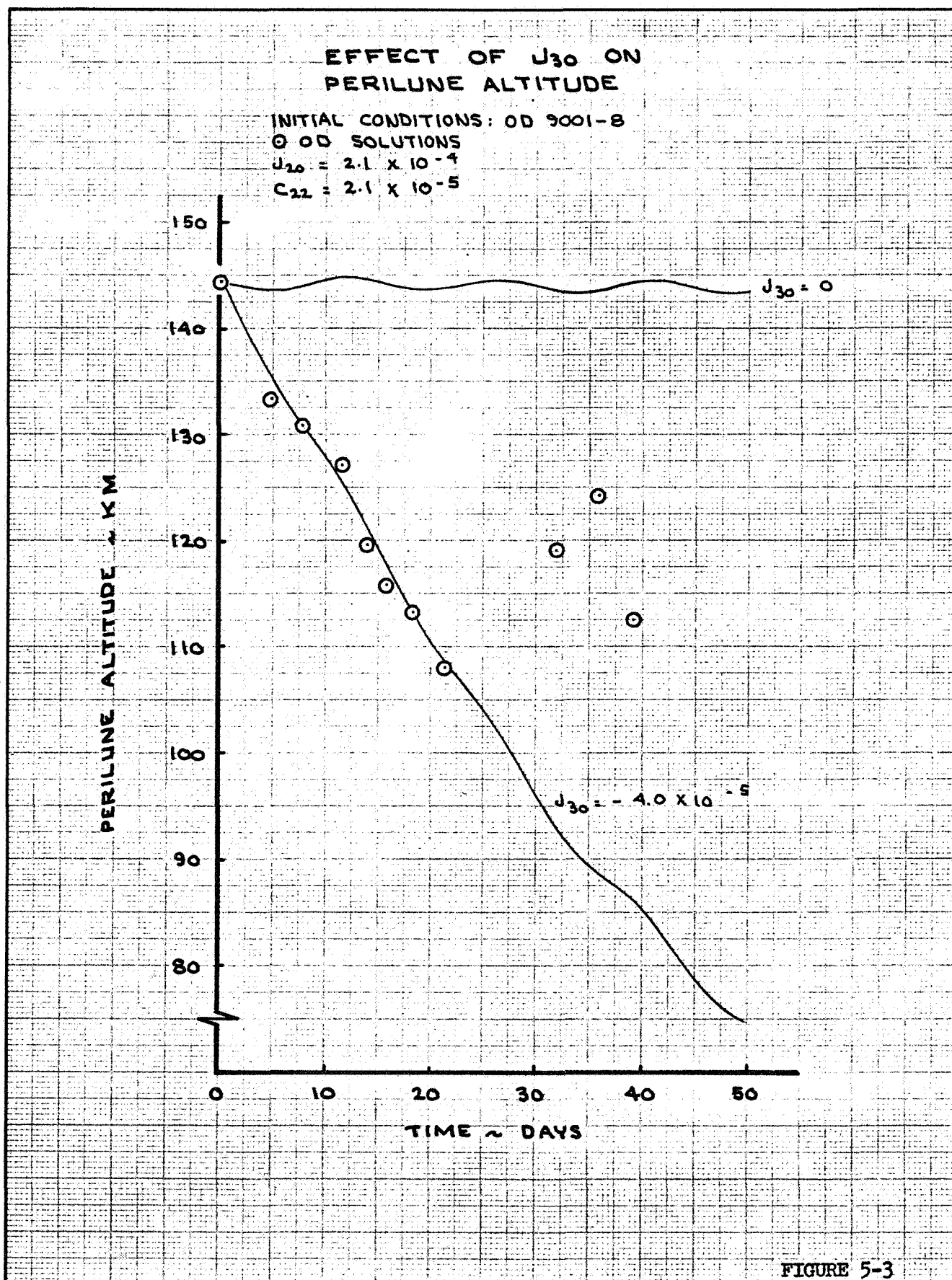


FIGURE 5-3

EFFECT OF J_{30} ON ORBIT INCLINATION

INITIAL CONDITIONS: 0 D 9001-8

0 D SOLUTIONS

$J_{20} = 2.1 \times 10^{-4}$

$C_{22} = 2.1 \times 10^{-5}$

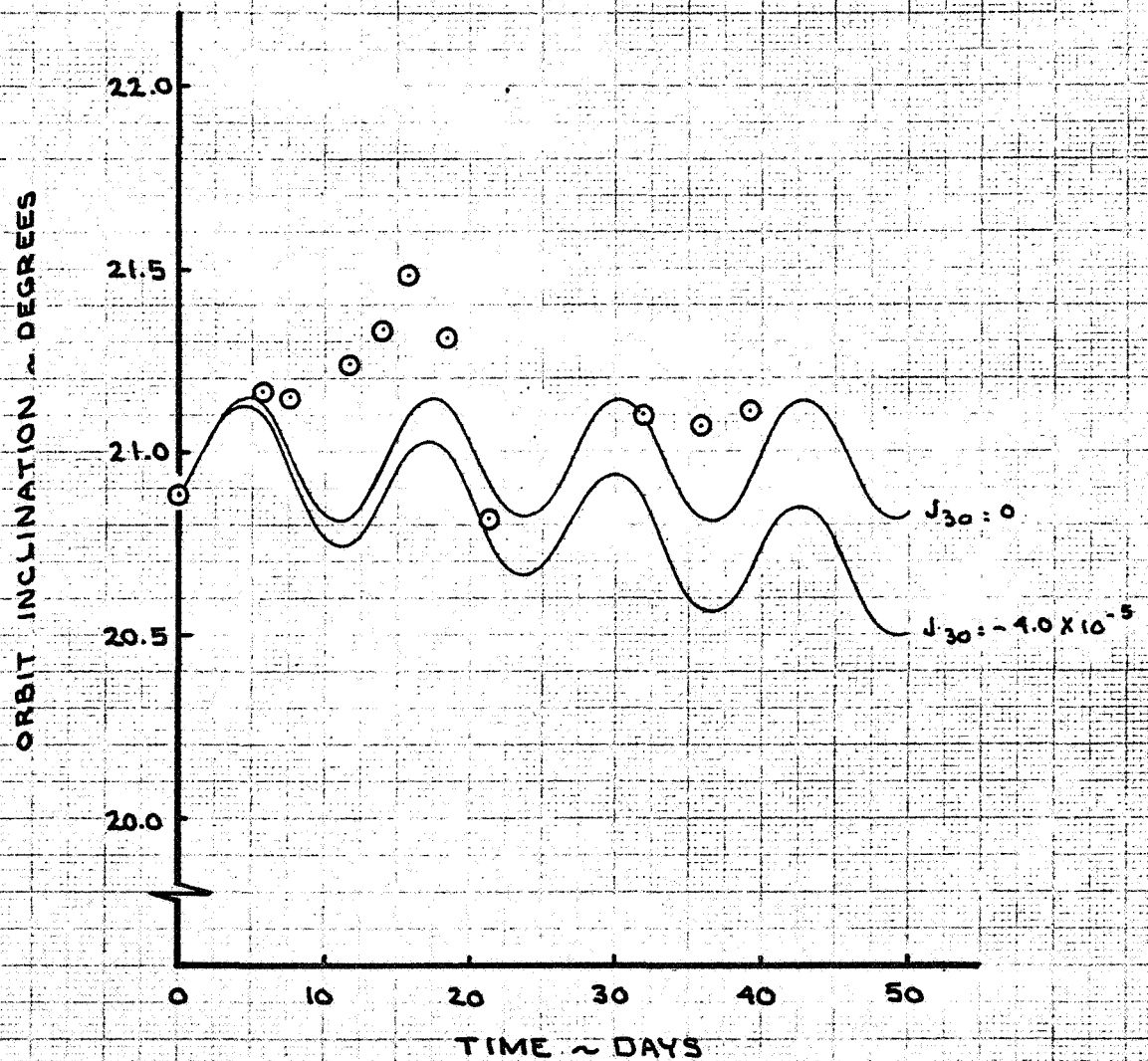


FIGURE 5-4

**EFFECT OF J_{40} ON
PERILUNE ALTITUDE**

INITIAL CONDITIONS : 0 D 9001-8

① 0D SOLUTIONS

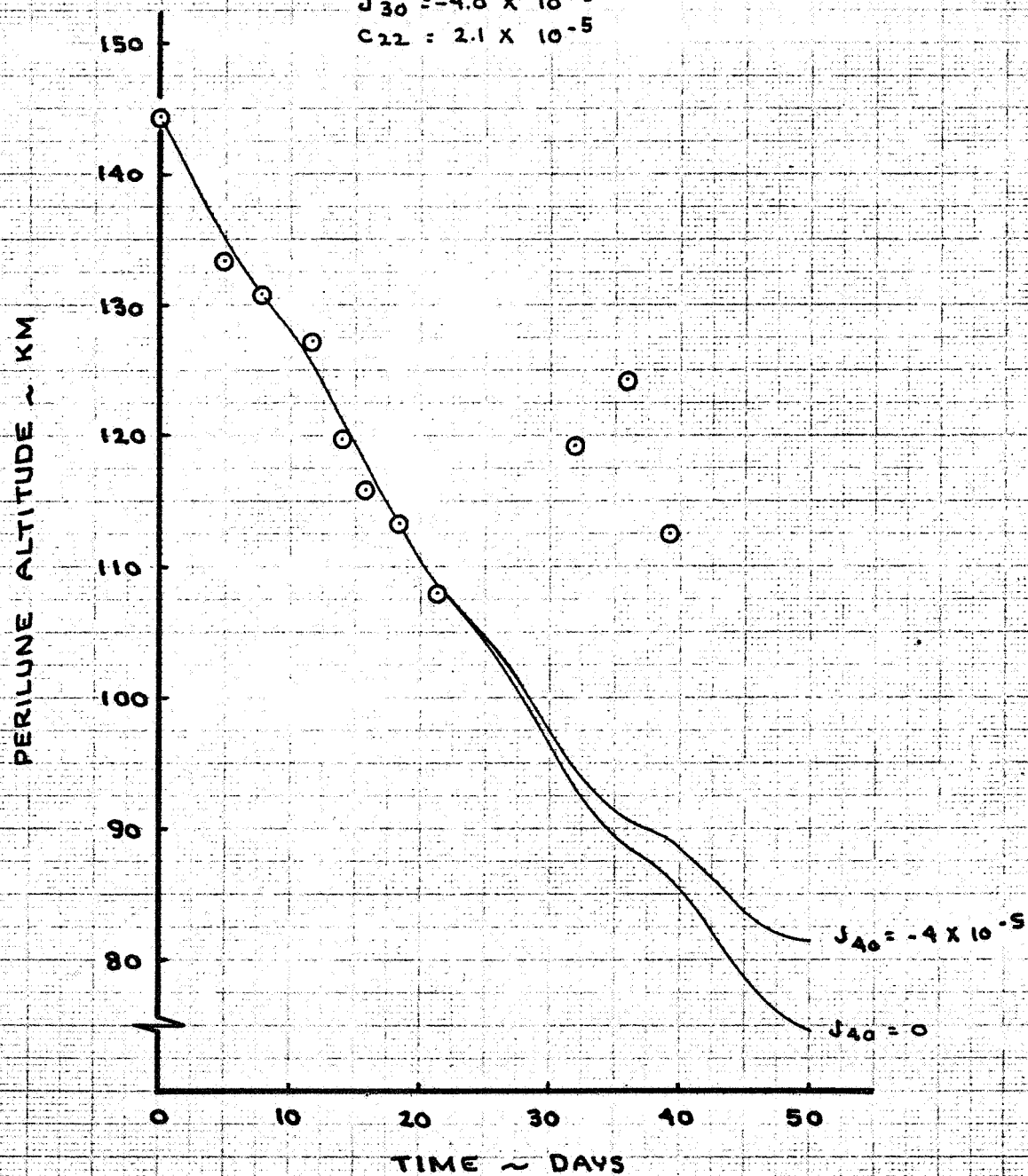
 $J_{20} = 2.1 \times 10^{-4}$ $J_{30} = -4.0 \times 10^{-5}$ $C_{22} = 2.1 \times 10^{-5}$ 

FIGURE 5-5

EFFECT OF J_{40} ON
NODE LONGITUDE

INITIAL CONDITIONS : OD 9001-8

O O D SOLUTIONS

$$J_{20} = 2.1 \times 10^{-4}$$

$$J_{30} = -4.0 \times 10^{-5}$$

$$C_{22} = 2.1 \times 10^{-5}$$

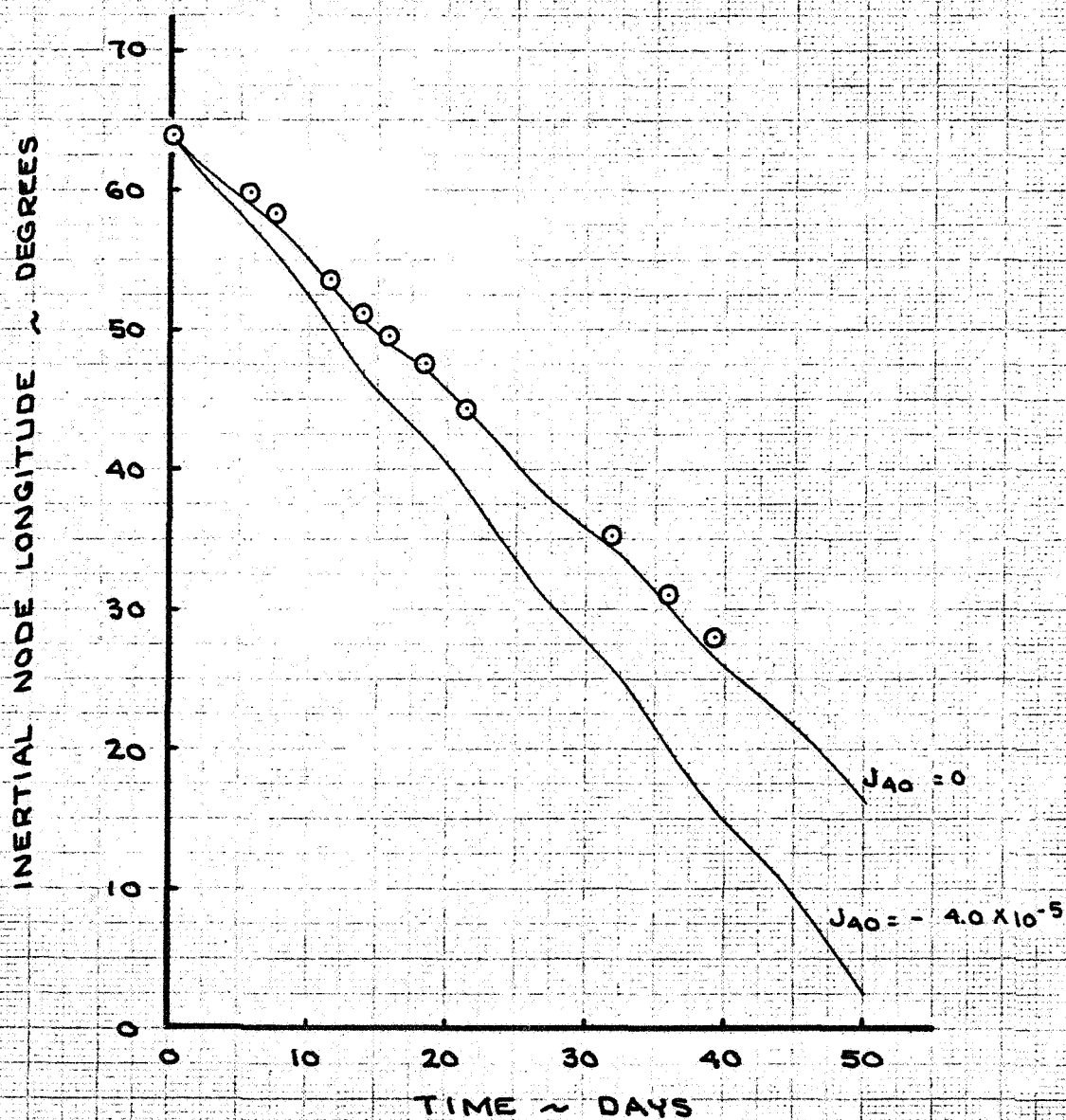


FIGURE 5-6

EFFECT OF J_{40} ON
ARGUMENT OF PERILUNE

INITIAL CONDITIONS: OD 9001-8

O OD SOLUTIONS

$$J_{20} = 2.1 \times 10^{-4}$$

$$J_{30} = -4.0 \times 10^{-5}$$

$$C_{12} = 2.1 \times 10^{-5}$$

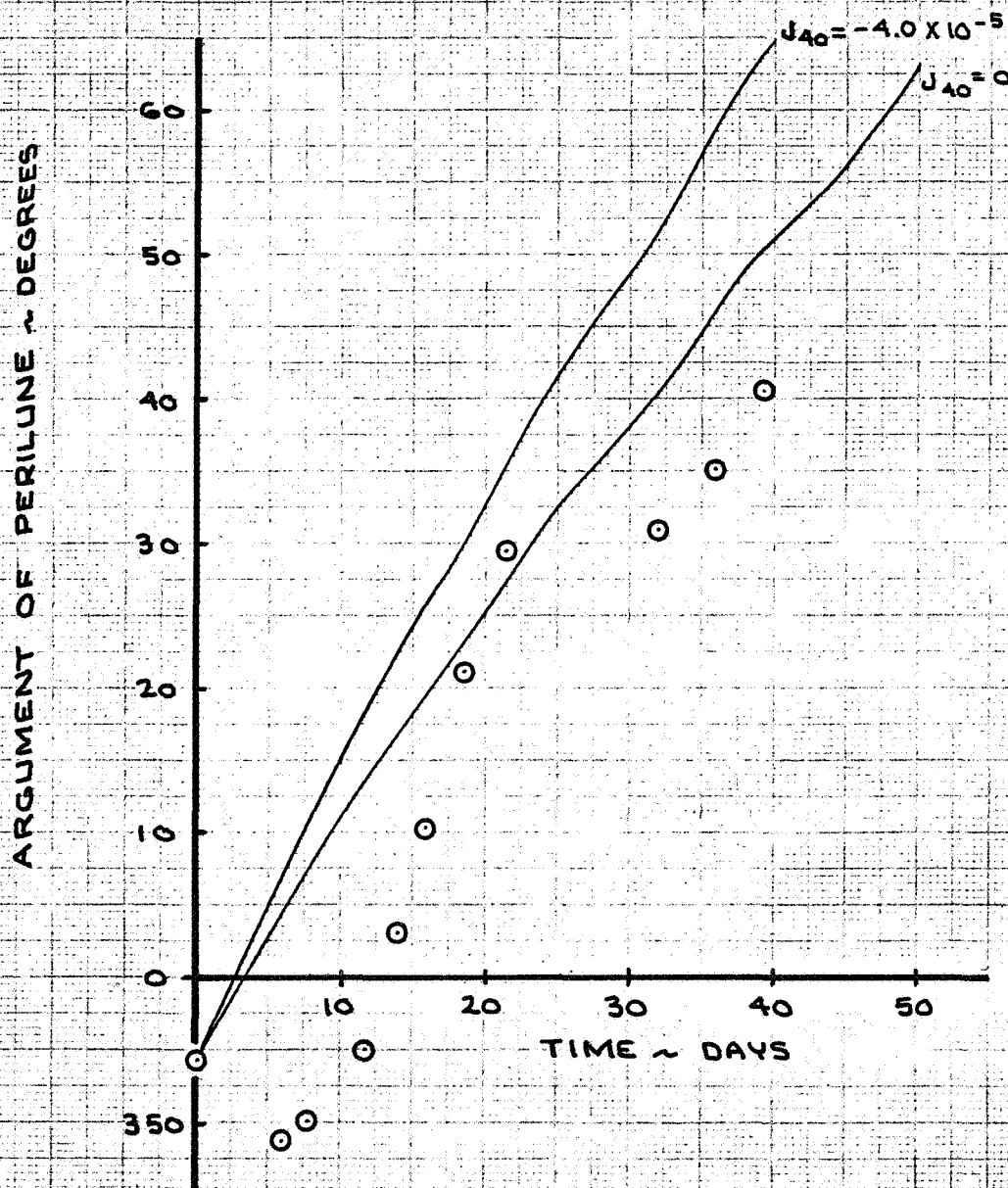


FIGURE 5-7

EFFECT OF C_{22} ON
ORBIT INCLINATION

INITIAL CONDITIONS: OD 9001-8

O O D SOLUTIONS

$$J_{20} = 2.1 \times 10^{-4}$$

$$J_{30} = -4.0 \times 10^{-5}$$

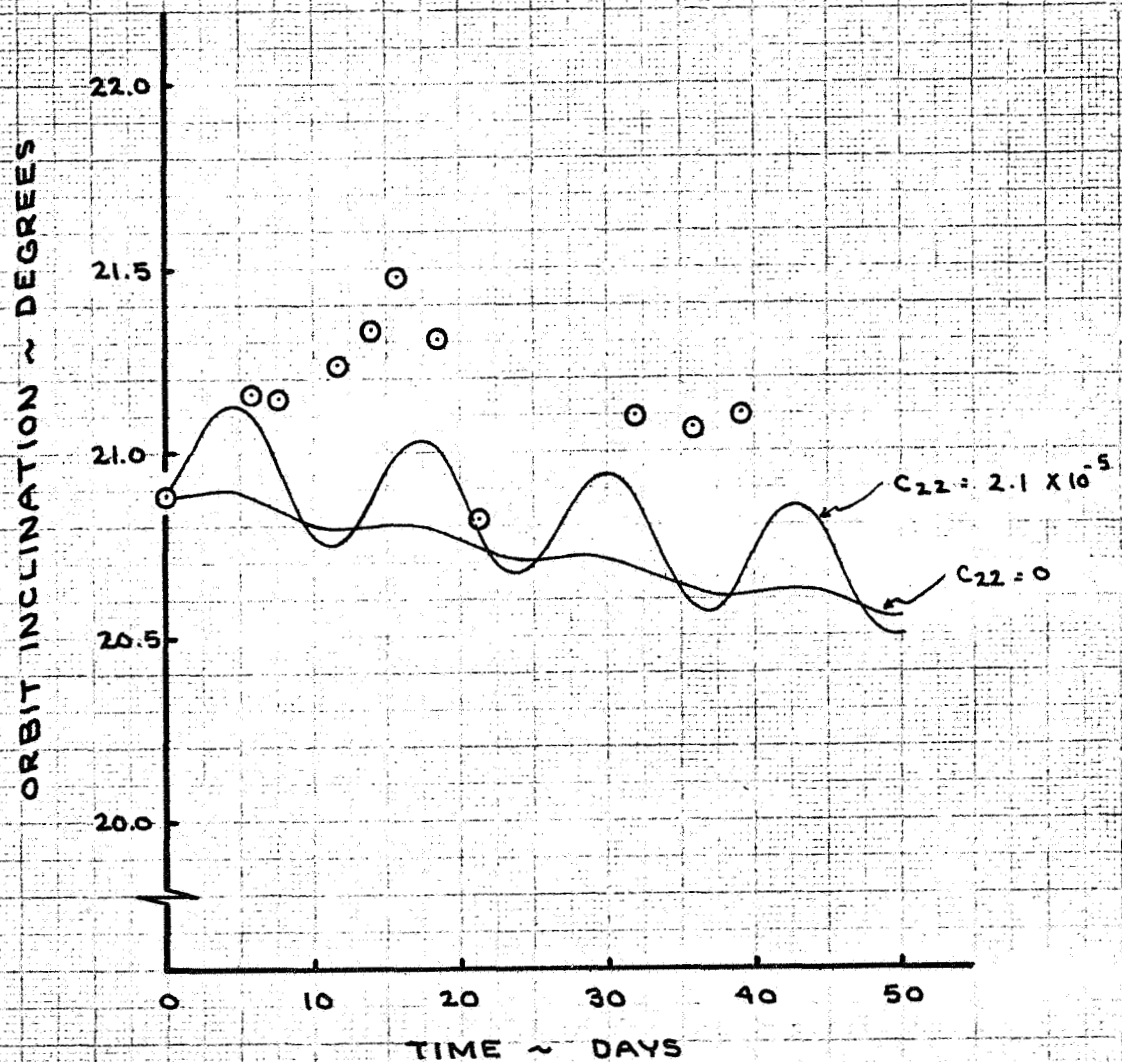


FIGURE 5-8

EFFECT OF C_{31} ON
PERILUNE ALTITUDE

INITIAL CONDITIONS: OD 9001-8
O OD SOLUTIONS
 $J_{20} = 2.07108 \times 10^{-4}$
 $J_{30} = -2.1 \times 10^{-5}$
 $C_{21} = 2.0716 \times 10^{-5}$

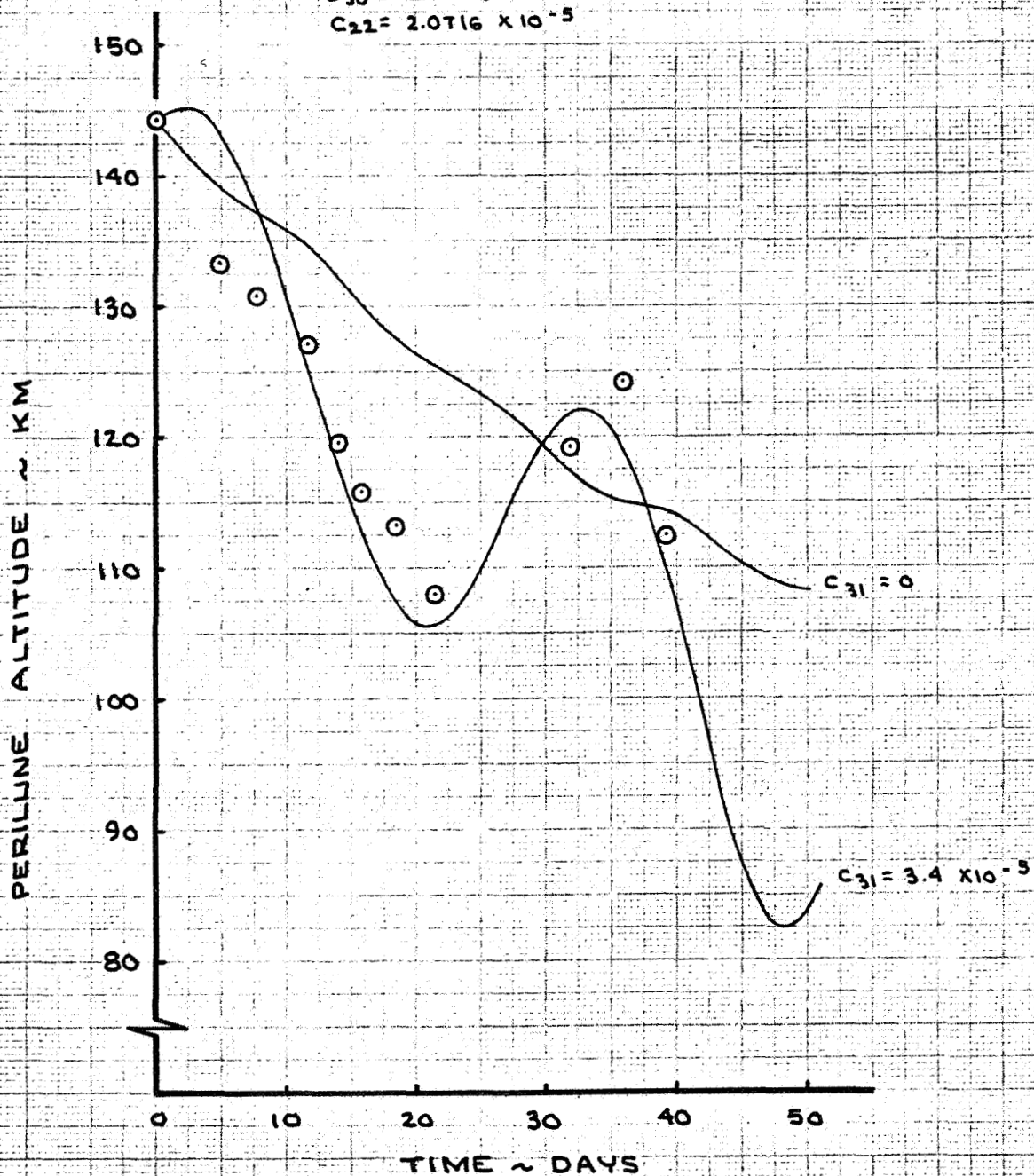


FIGURE 5-9

EFFECT OF C_{31} ON
ARGUMENT OF PERILUNE

INITIAL CONDITIONS: 00 9001-8

① OD SOLUTIONS

$$J_{20} = 2.07108 \times 10^{-4}$$

$$J_{30} = -2.1 \times 10^{-5}$$

$$C_{22} = 2.0716 \times 10^{-5}$$

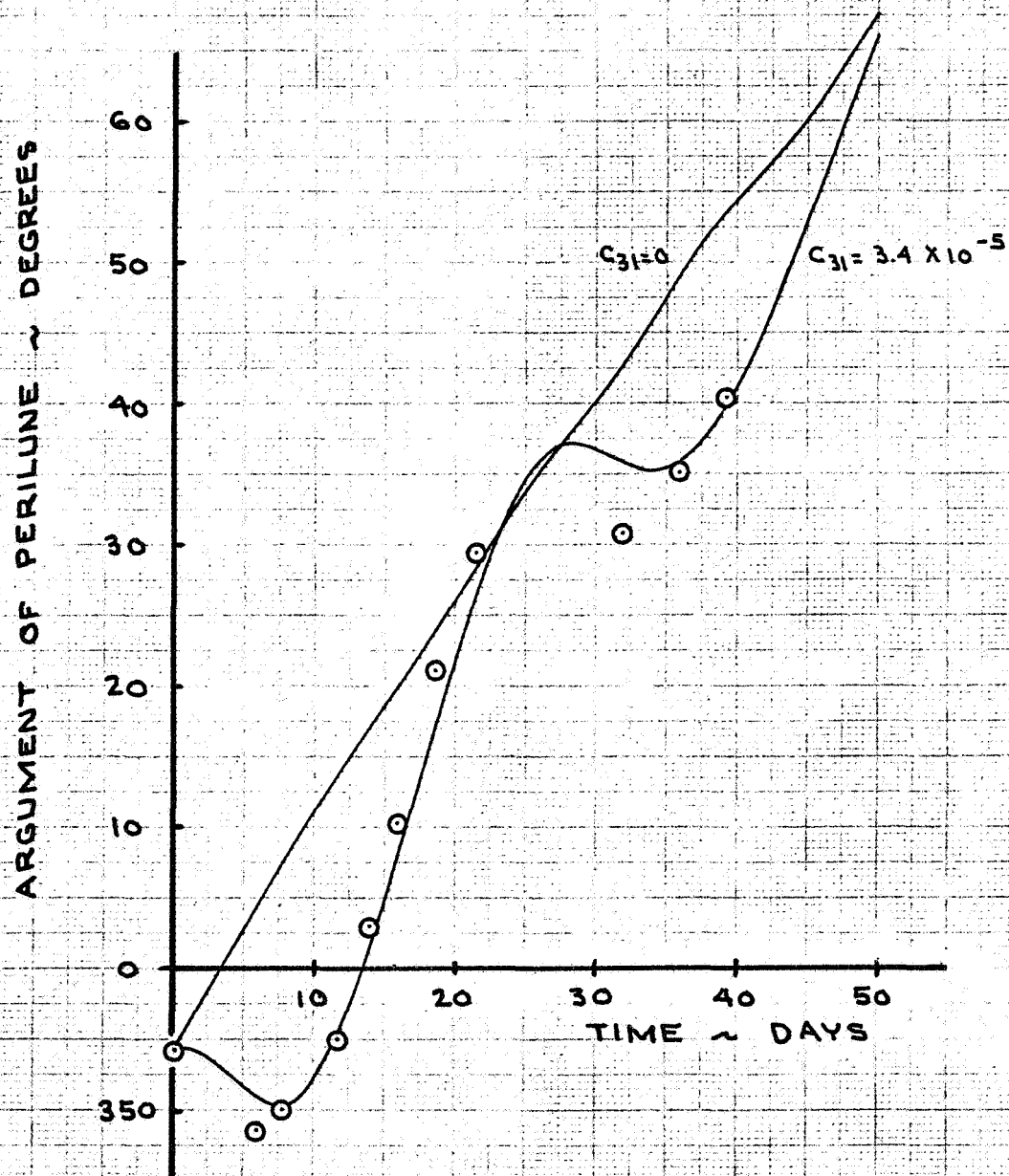


FIGURE 5-10

6.0 CHARACTERISTICS OF SIMPLE LUNAR MODELS

Orbit element histories are shown for two simple lunar gravitational models; a preliminary model designated R-1 and the recommended model R-2.

6.1 PRELIMINARY R-1 MODEL

During the early phase of the study, a preliminary model was developed which consists of the coefficients J_{20} , J_{30} , J_{40} , and C_{22} . Although this model proved to be unsatisfactory, it is included to provide a complete report on the work which was accomplished. This R-1 model is defined as follows:

$$\begin{aligned}J_{20} &= 2.1 \times 10^{-4} \\J_{30} &= -4.0 \times 10^{-5} \\J_{40} &= 0 \\C_{22} &= 2.1 \times 10^{-5}\end{aligned}$$

These coefficients are used in the orbit perturbation equations as defined in the Appendix. These values provide the best fit of the Lunar Orbiter III, Phase 9, tracking data when the model is limited to these coefficients.

The value of J_{30} was adjusted to -4.0×10^{-5} to obtain a good fit of perilune altitude for the first 22 days. The value of J_{40} was set at 0 since this coefficient provided no improvements in any of the data. A value of 2.1×10^{-4} was defined for J_{20} to provide a good fit of node longitude. This value is essentially that of the triaxial moon model. For C_{22} , a value of 2.1×10^{-5} was selected as this is essentially that of the triaxial moon model and it provides a reasonable variation in orbit inclination.

Orbit element histories as predicted with the preliminary model R-1 are presented in Figures 6-1 through 6-4. Initial conditions are taken as those of OD 9001-8 (see Table 6-1). These histories are compared with actual OD solutions from Lunar Orbiter III, Phase 9 tracking data.

This model, R-1, is considered as unsatisfactory as it does not follow the trend in perilune altitude (see Figure 6-1). Also, there are large errors in argument of perilune (Figure 6-3). The model was defined during the early phase of the study as the best model obtainable within the limits of the 4 coefficients considered. When it became apparent that this model was unsatisfactory, the R-2 model was developed (utilizing one other coefficient).

6.2 R-2 MODEL

The R-2 model is defined as follows:

$$\begin{aligned}J_{20} &= 2.07108 \times 10^{-4} \\J_{30} &= -2.1 \times 10^{-5} \\C_{22} &= 2.0716 \times 10^{-5} \\C_{31} &= 3.4 \times 10^{-5}\end{aligned}$$

USE FOR TYPEWRITTEN MATERIAL ONLY

These coefficients are used in the orbit perturbation equations as defined in the Appendix.

For this model, J_{20} and C_{22} were assigned the values of the triaxial moon model since it had been determined during the development of the R-1 model that these values were satisfactory. The values of J_{30} and C_{31} were then adjusted to obtain the best fit of perilune altitude and argument of perilune with the data from Lunar Orbiter III, Phase 9. The model was then checked against data from Phase 6 of Lunar Orbiter III and slight adjustments were made in both J_{30} and C_{31} to improve the fit while not degrading the fit with the Phase 9 data.

Orbit element variations as predicted with the R-2 model are compared with tracking data (OD solutions) from 5 different orbit phases of the Lunar Orbiter missions.

Lunar Orbiter III, Phase 9 Comparisons are presented in Figures 6-5 through 6-8. The initial conditions used are those of OD 9001-8 (defined in Table 6-1) which was the first orbit determination obtained after the orbit was adjusted to simulate the Apollo orbit. This is a near circular orbit with an inclination of about 21° .

Orbit element variations as predicted with the triaxial moon model are included for comparison with the R-2 model results. It is noted that the R-2 model is far superior to the triaxial moon model. A very good prediction of perilune altitude is obtained. Node longitude prediction is excellent, and argument of perilune is predicted very well. The prediction in orbit inclination appears reasonable, considering the apparent scatter in the data.

Lunar Orbiter III, Phase 6 Comparisons are presented in Figures 6-9 through 6-12. Phase 6 was the first phase after completion of photography. The orbit is elliptical with an inclination of about 21° . Table 6-1 defines the initial conditions (OD 6000-8) used in the comparisons.

With an examination of the results given in Figures 6-9 through 6-12, it is seen that a good overall fit is obtained for each of the 4 elements.

Lunar Orbiter III, Phase 5 Comparisons are presented in Figures 6-13 through 6-16. These data are presented to demonstrate the short term fit. A phase was selected that had a large number of data points; at least 2 per day. Phase 5 is the photographic phase of Lunar Orbiter III; its characteristics are nearly the same as those of Phase 6. (See OD 5302-8 in Table 6-1.) The first 4 days of the phase are shown as this time period is representative of the maximum orbital duration of an Apollo mission.

An excellent fit is obtained for all the orbit elements over the 4 day period shown.

Lunar Orbiter I Comparisons are presented in Figures 6-17 through 6-20. This orbit has approximately the same altitude as the early phases of Lunar Orbiter III, with an inclination of about 12° (OD 7000-4, Table 6-1).

USE FOR TYPEWRITTEN MATERIAL ONLY

Lunar Orbiter V Comparisons are presented in Figures 6-21 through 6-24. This is an elliptical orbit with an inclination of 85° . (See OD 8000-10, Table 6-1). A very good fit is obtained for all 4 orbit elements over the complete time period of 110 days. The excellent fit of the orbit inclination data (Figure 6-24) indicates that there is very little scatter in the data and that the value of C_{22} is valid. (Previous inclination data shown did not indicate a very good fit due to scatter in the data.) It is significant to note that the model which was developed for an orbit with a low inclination (21°) and nearly circular (eccentricity = 0.04) is also valid for the Lunar Orbiter V orbit (inclination = 85° , eccentricity = 0.3).

USE FOR TYPEWRITTEN MATERIAL ONLY

USE FOR TYPEWRITTEN MATERIAL ONLY

Table 6-1
INITIAL CONDITIONS

IDENTIFICATION	OD9001-8	OD6000-8	OD5302-8	OD7000-4	OD8000-10
LUNAR ORBITER	III	III	III	I	V
PHASE	9	6	5	7	8
EPOCH					
DATE:					
TIME (HR, MIN) GMT	8-30-67	2-24-67	2-12-67	9-14-66	10-10-67
APOLUNE ALTITUDE, KM	20:55	4:10	18:14	6:00	19:40
PERILUNE ALTITUDE, KM	315.29	1842.30	1847.15	1813.74	1985.88
ORBIT INCLINATION, DEG.	144.46	57.69	54.92	48.79	200.13
NODE LONGITUDE (SELENOGRAPHIC), DEG.	20.88	20.82	20.86	12.22	85.15
ARGUMENT OF PERILUNE, DEG.	63.93	103.99	258.75	268.21	323.87
	354.31	185.55	178.12	206.41	12.06

PERILUNE ALTITUDE HISTORY
LUNAR ORBITER III - PHASE 9

INITIAL CONDITIONS: OD 9001-8

○ OD SOLUTIONS

— MODEL R-1

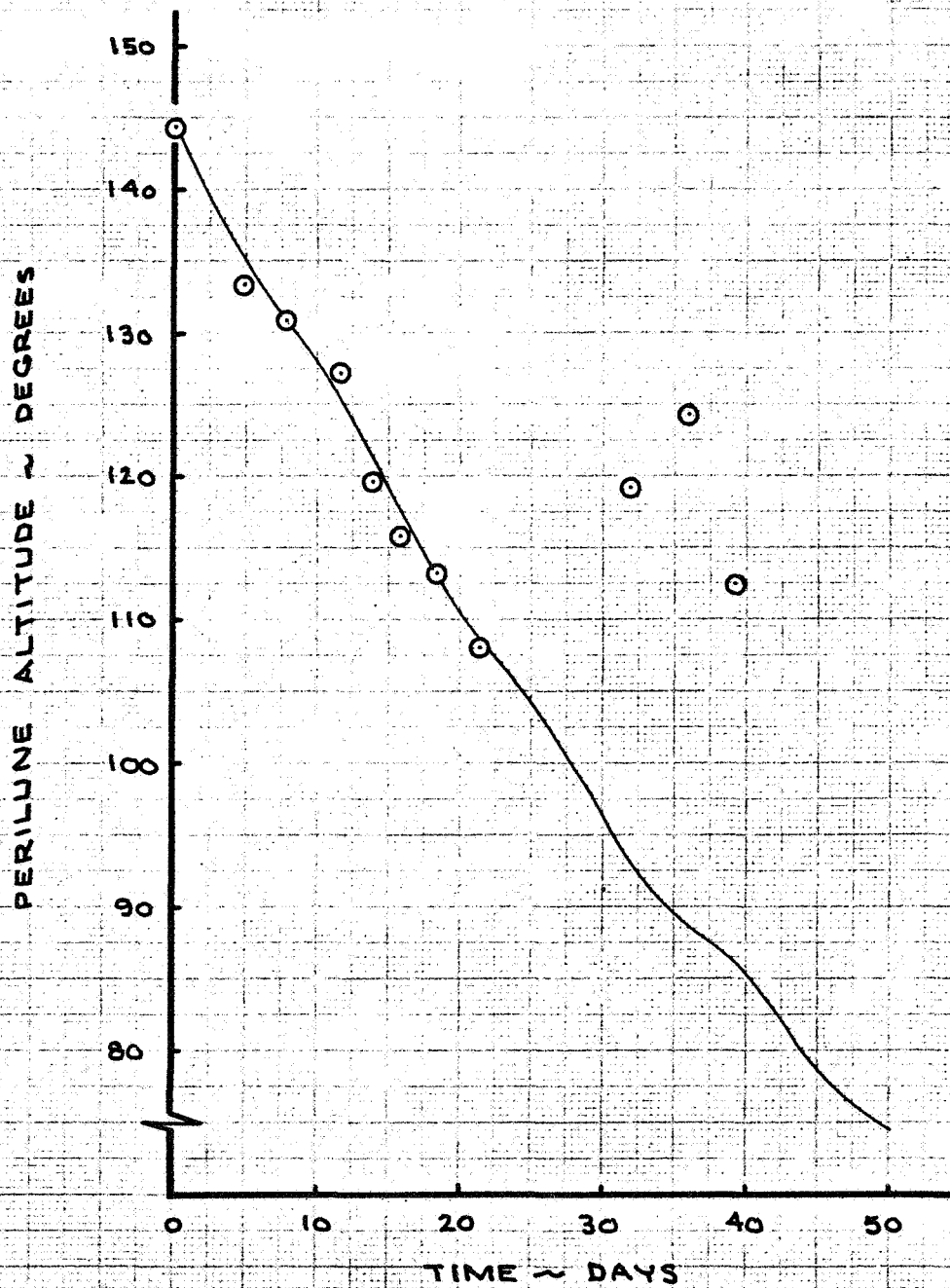


FIGURE 6-1

NODE LONGITUDE HISTORY
LUNAR ORBITER III - PHASE 9

INITIAL CONDITIONS : OD 9001-8

○ OD SOLUTIONS

— MODEL R-1

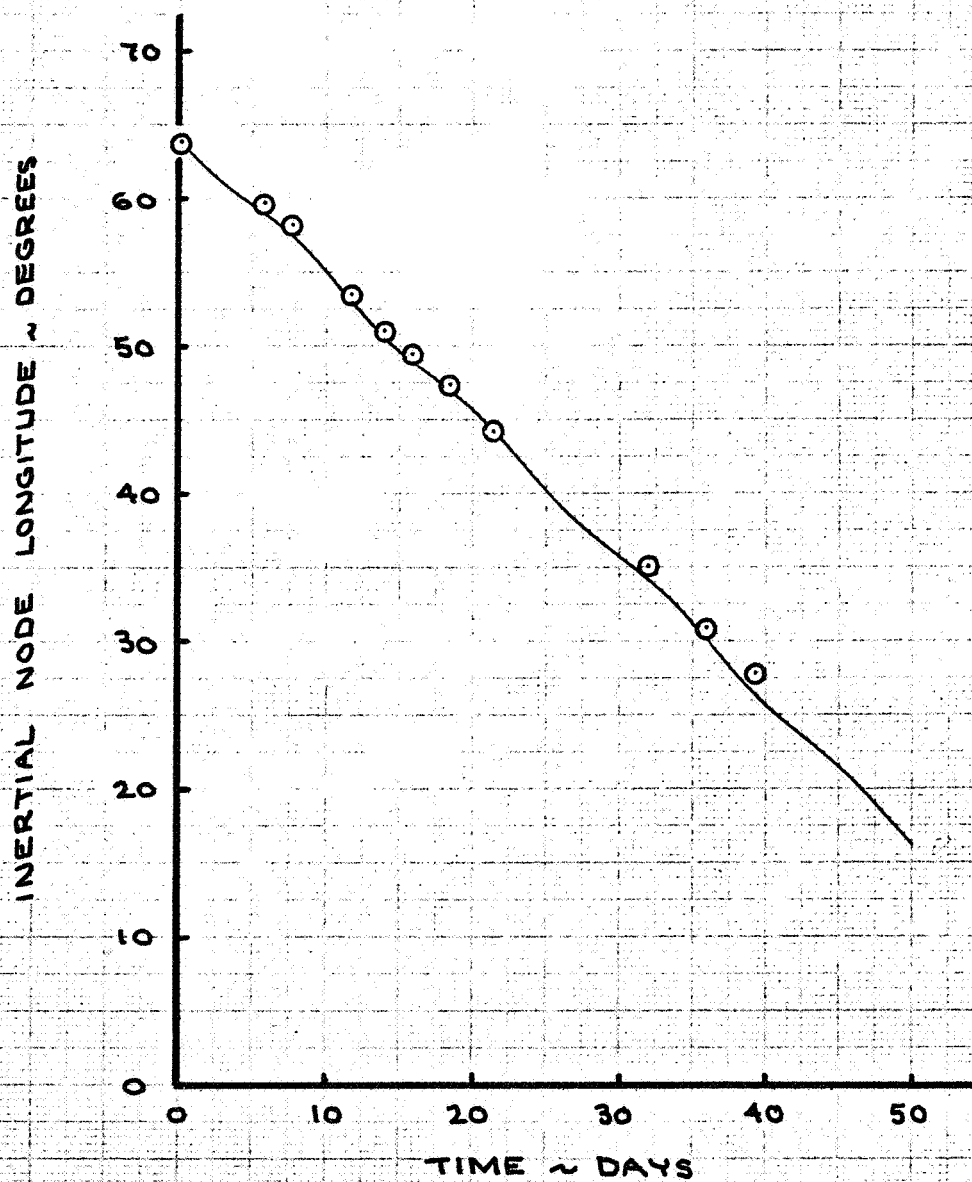


FIGURE 6-2

ARGUMENT OF PERILUNE HISTORY
LUNAR ORBITER III - PHASE 9

INITIAL CONDITIONS: OD 9001-8

⊙ OD SOLUTIONS

— MODEL R-1

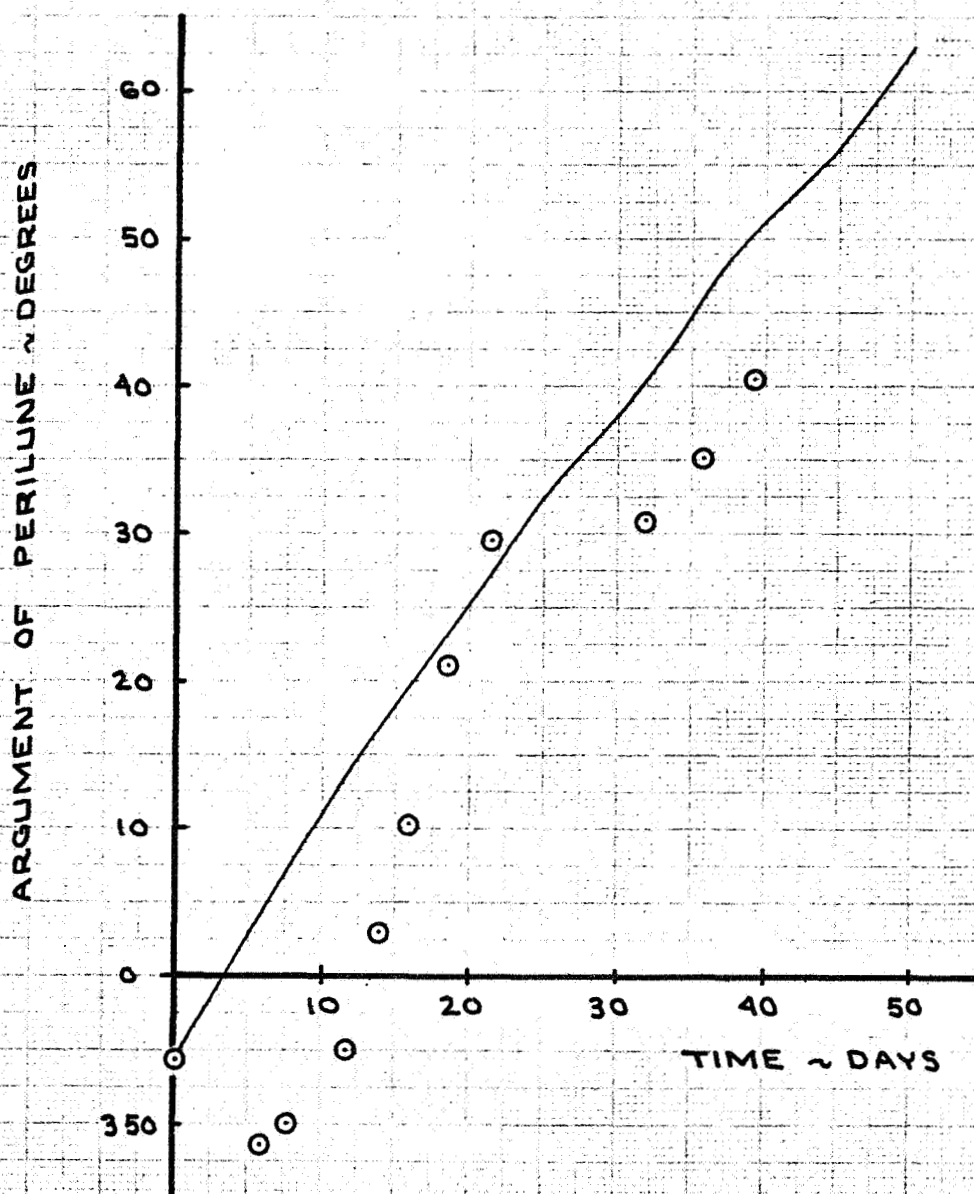


FIGURE 6-3

ORBIT INCLINATION HISTORY
LUNAR ORBITER III PHASE 9

INITIAL CONDITIONS: OD 9001 - 8

○ OD SOLUTIONS

— MODEL R-1

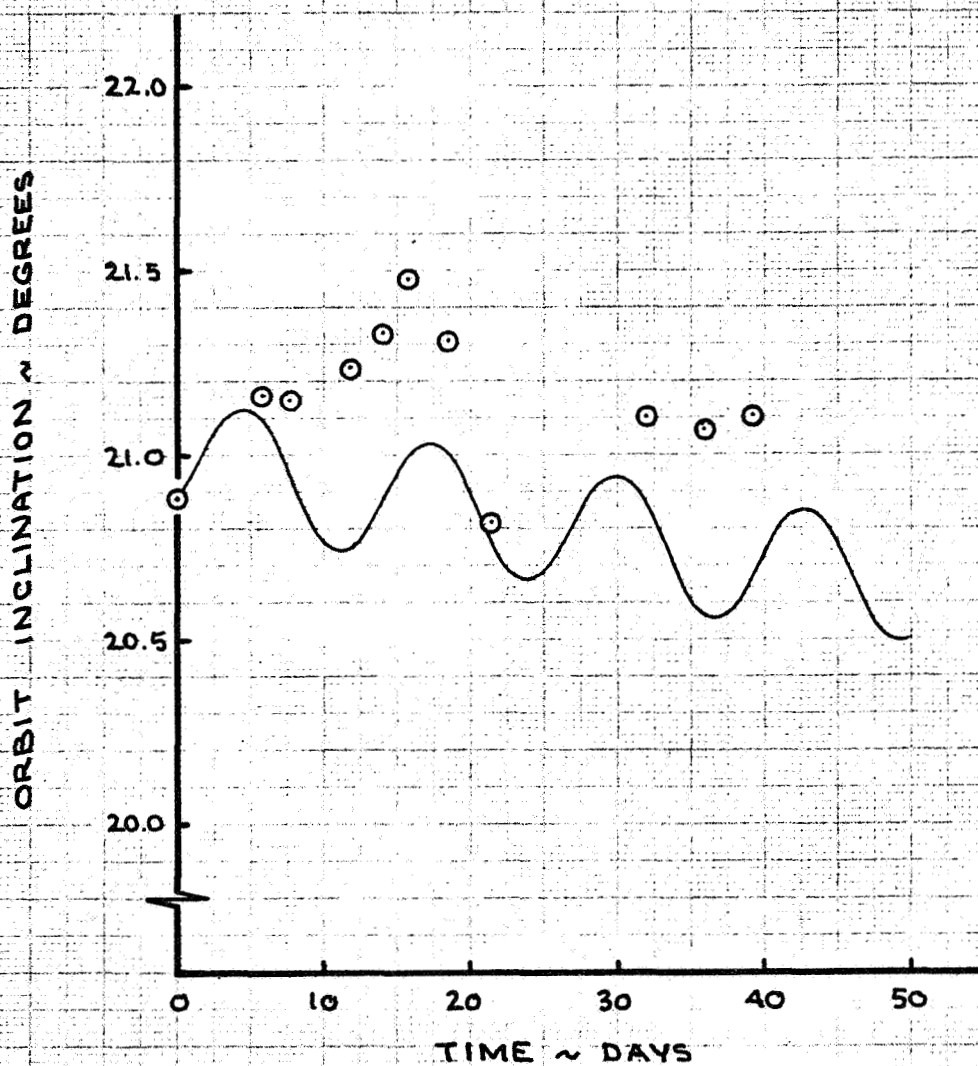


FIGURE 6-4

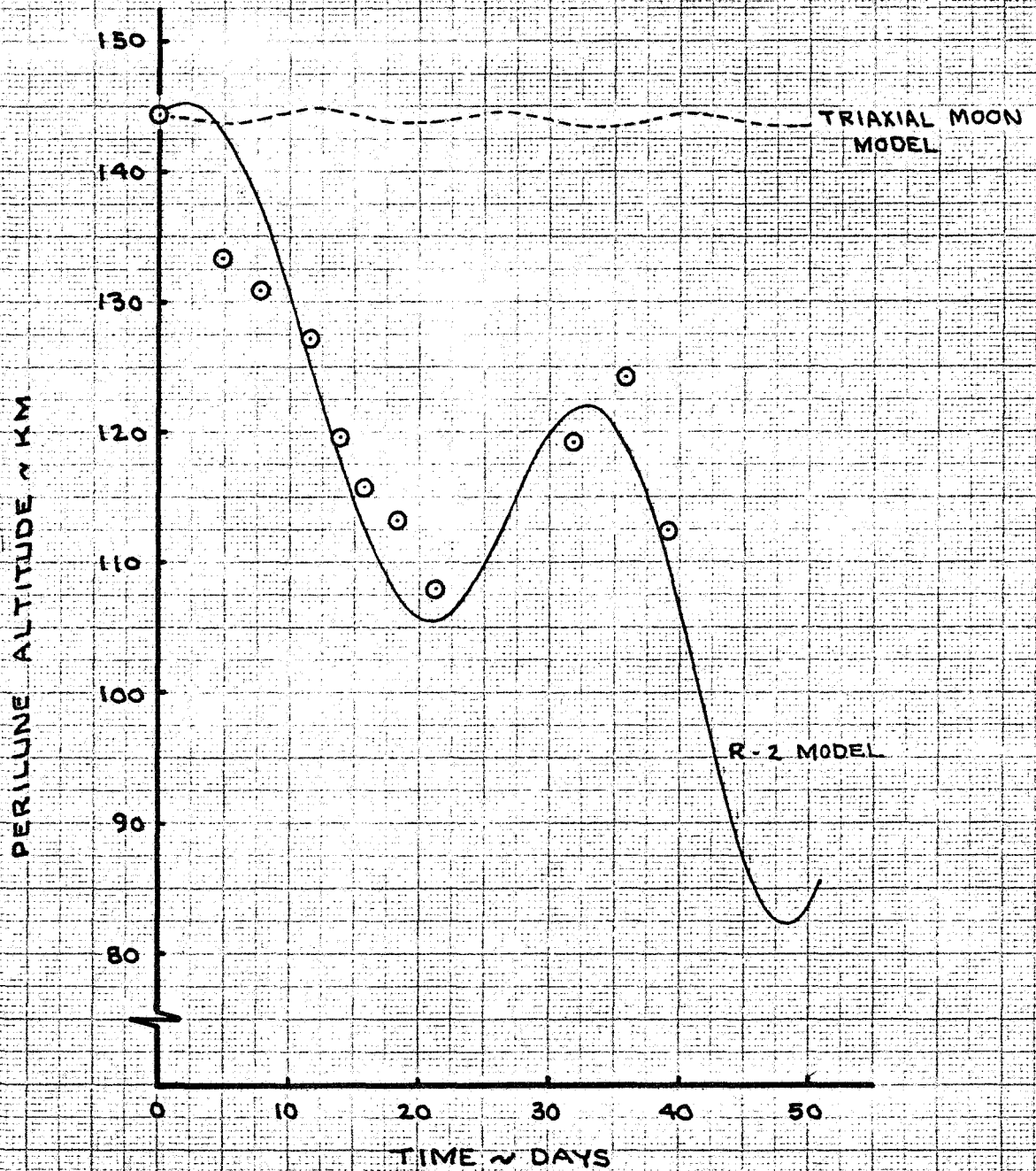
PERILUNE ALTITUDE HISTORY
LUNAR ORBITER III, PHASE 9INITIAL CONDITIONS: OD 9001-8
000 SOLUTIONS

FIGURE 6-5

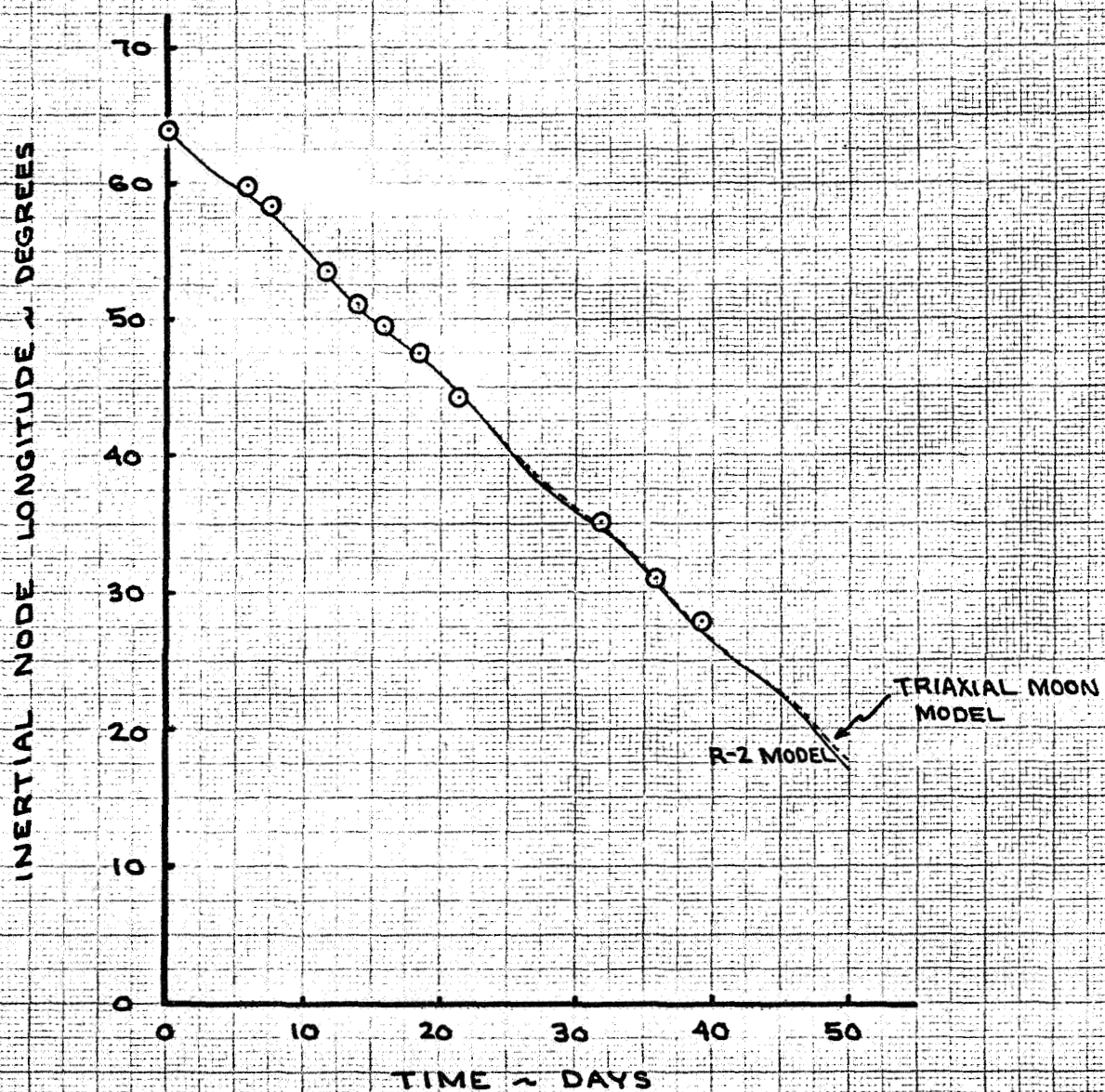
NODE LONGITUDE HISTORY
LUNAR ORBITER III - PHASE 9INITIAL CONDITIONS: OD 9001-8
O O D SOLUTIONS

FIGURE 6-6

ARGUMENT OF PERILUNE HISTORY LUNAR ORBITER III - PHASE 9

INITIAL CONDITIONS 00 9001-8
000 SOLUTIONS

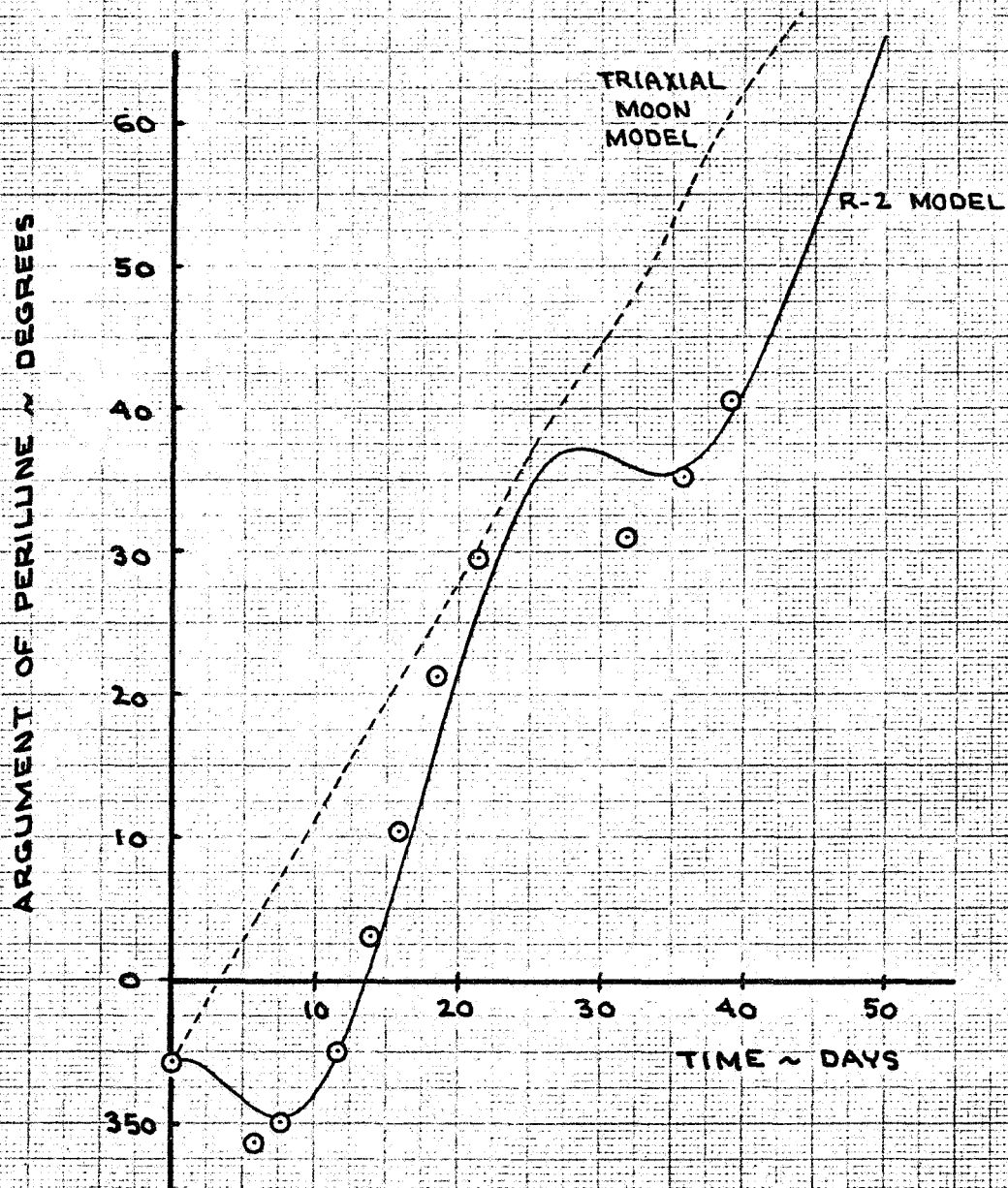


FIGURE 6-7

ORBIT INCLINATION HISTORY LUNAR ORBITER III - PHASE 9

INITIAL CONDITIONS: OD 9001-8
O O D SOLUTIONS

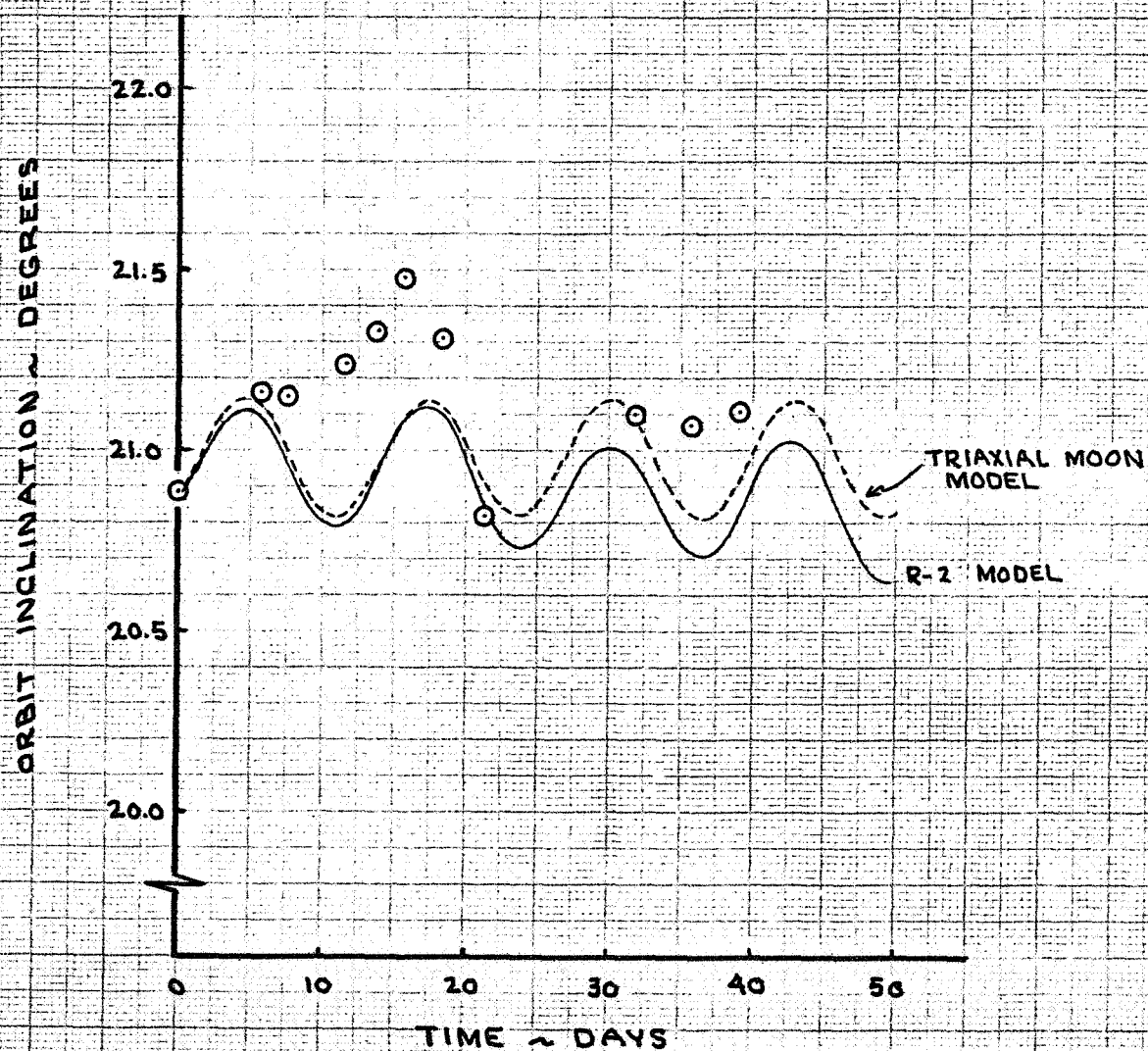


FIGURE 6-8

PERILUNE ALTITUDE HISTORY LUNAR ORBITER III - PHASE 6

INITIAL CONDITIONS: OD 6000 - 8

○ OD SOLUTIONS

— MODEL R-2

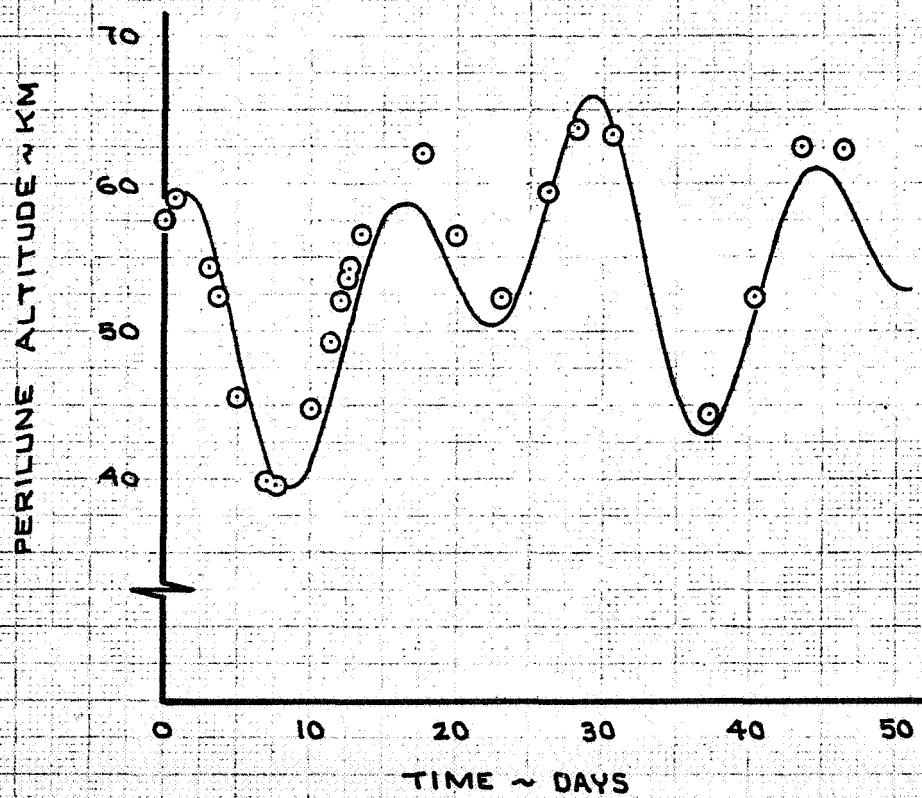


FIGURE 6-9

NODE LONGITUDE HISTORY
LUNAR ORBITER III - PHASE 6

INITIAL CONDITIONS : OD 6000 - 8

O OD SOLUTIONS

— MODEL R-2

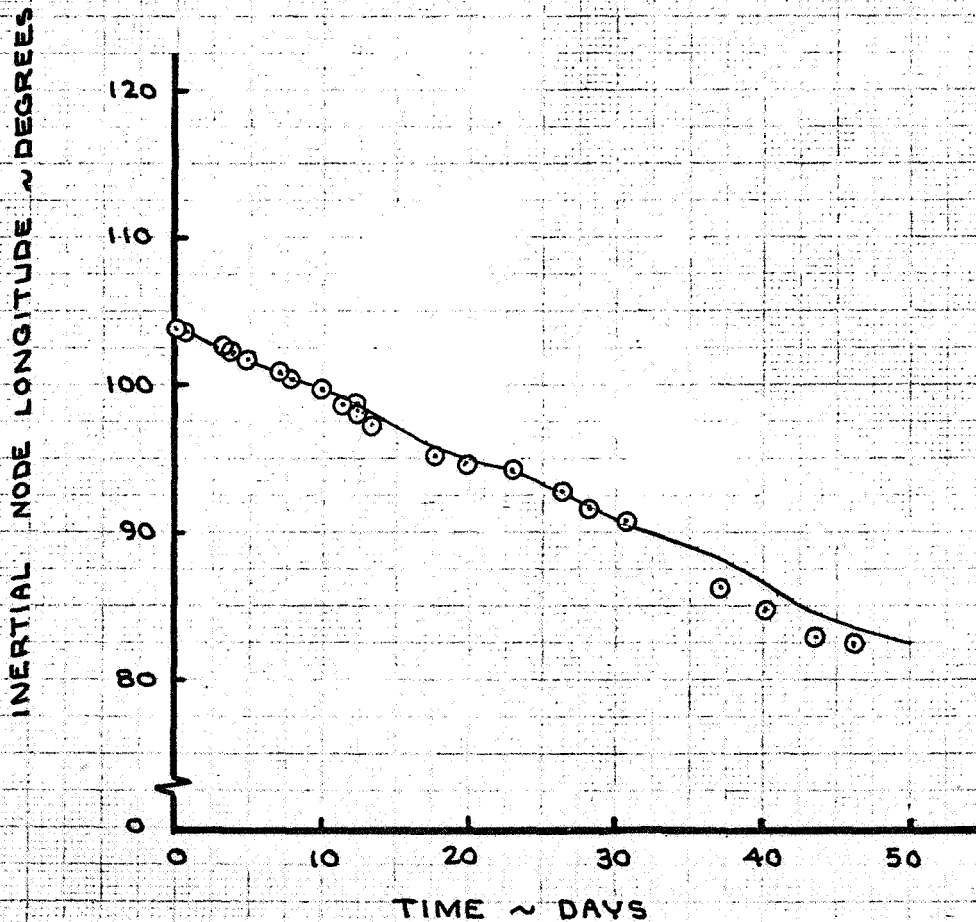


FIGURE 6-10

ARGUMENT OF PERILUNE HISTORY
LUNAR ORBITER III - PHASE G

INITIAL CONDITIONS: OD 6000-8

O O D SOLUTIONS

— MODEL R-2

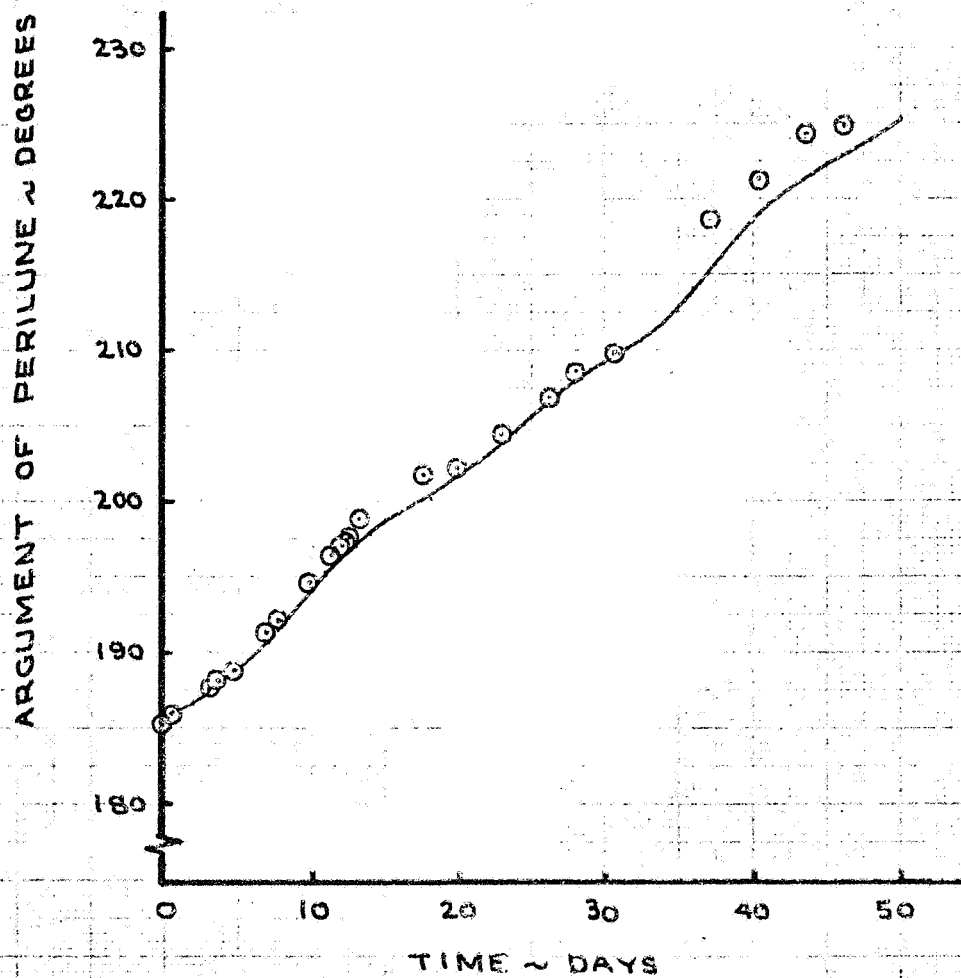


FIGURE 6-11

ORBIT INCLINATION HISTORY LUNAR ORBITER III - PHASE 6

INITIAL CONDITIONS: OD 6000-8

○ OD SOLUTIONS

— MODEL R-2

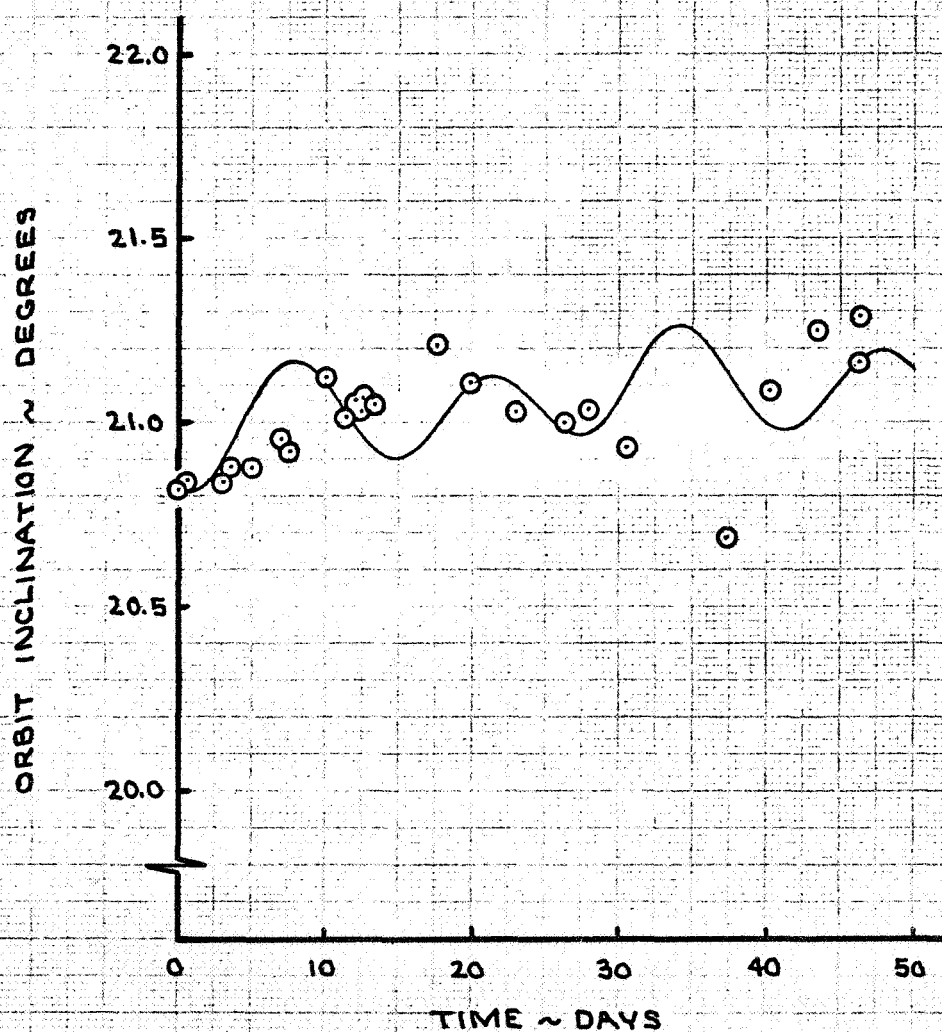


FIGURE 6-12

PERILUNE ALTITUDE HISTORY LUNAR ORBITER III - PHASE 5

INITIAL CONDITIONS: OD 5302-B

○ OD SOLUTIONS

— R-2 MODEL

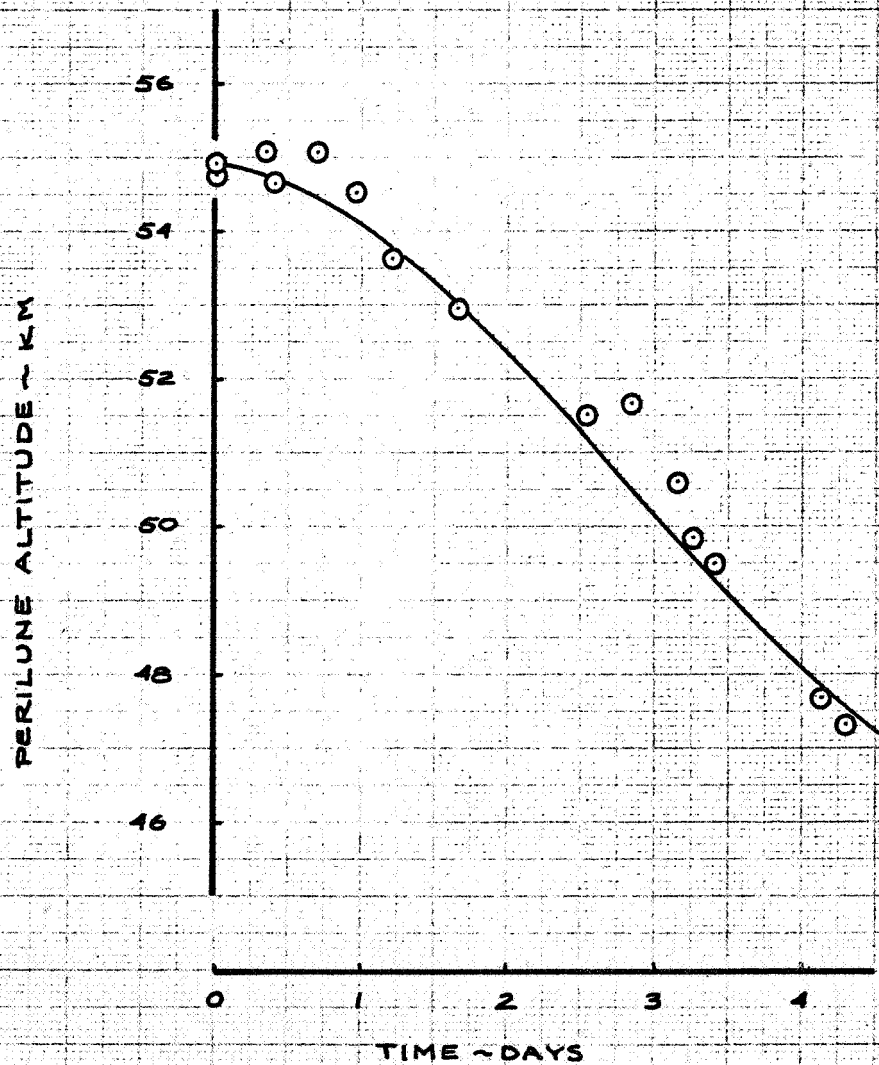


FIGURE 6-13

NODE LONGITUDE HISTORY
LUNAR ORBITER III - PHASE 5

INITIAL CONDITIONS: OD 5302-B

○ OD SOLUTIONS

— R-2 MODEL

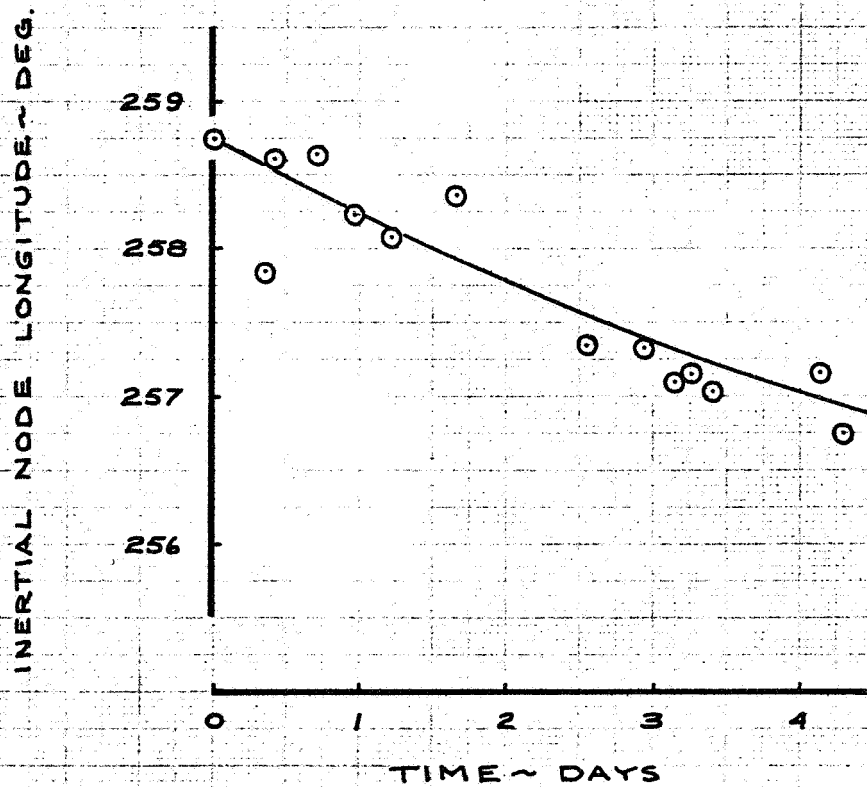


FIGURE 6-14

ARGUMENT OF PERILUNE HISTORY
LUNAR ORBITER III - PHASE 5

INITIAL CONDITIONS: OD 5302-8

○ OD SOLUTIONS

— R-2 MODEL

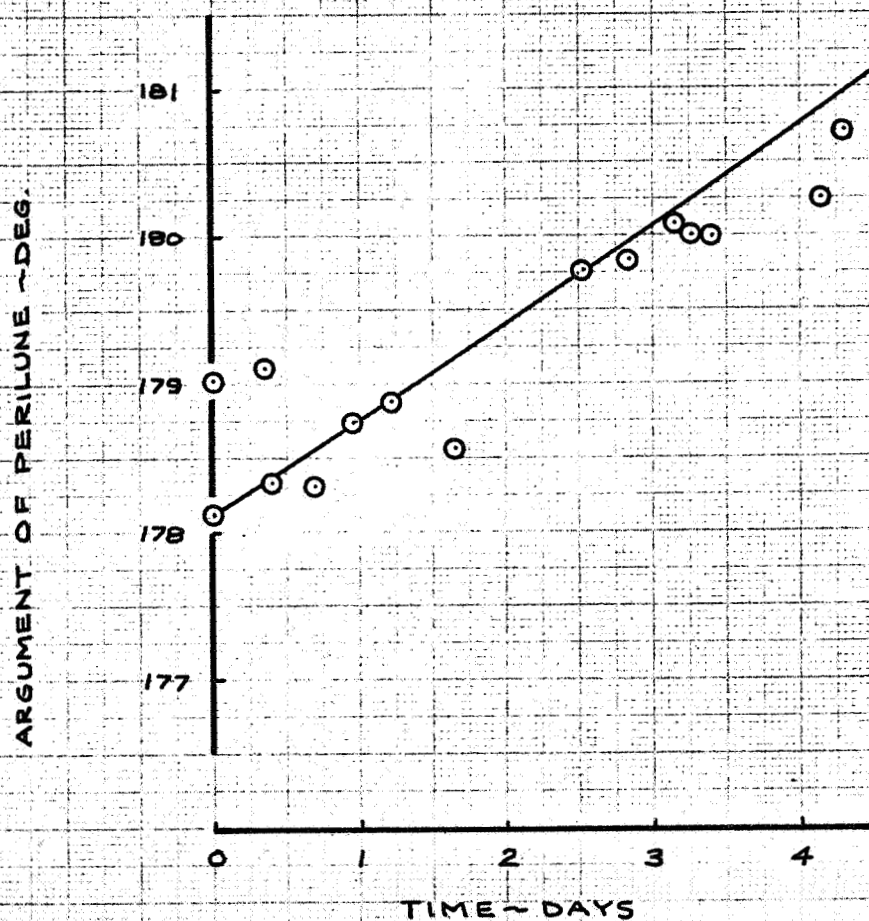


FIGURE 6-15

**ORBIT INCLINATION HISTORY
LUNAR ORBITER III - PHASE 5**

INITIAL CONDITIONS: OD 5302-B

○ OD SOLUTIONS

— R-2 MODEL

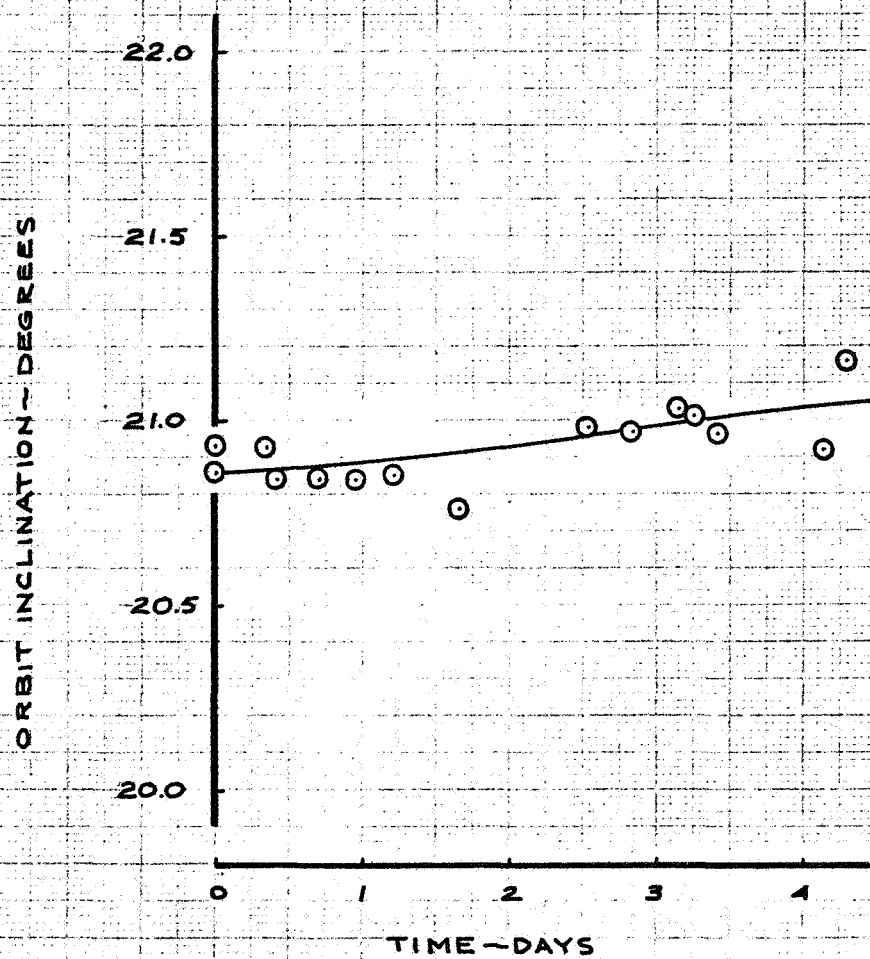


FIGURE 6-16

PERILUNE ALTITUDE HISTORY
LUNAR ORBITER I - PHASE T

INITIAL CONDITIONS : O D 7000-4

⊙ OD SOLUTIONS

— MODEL R-2

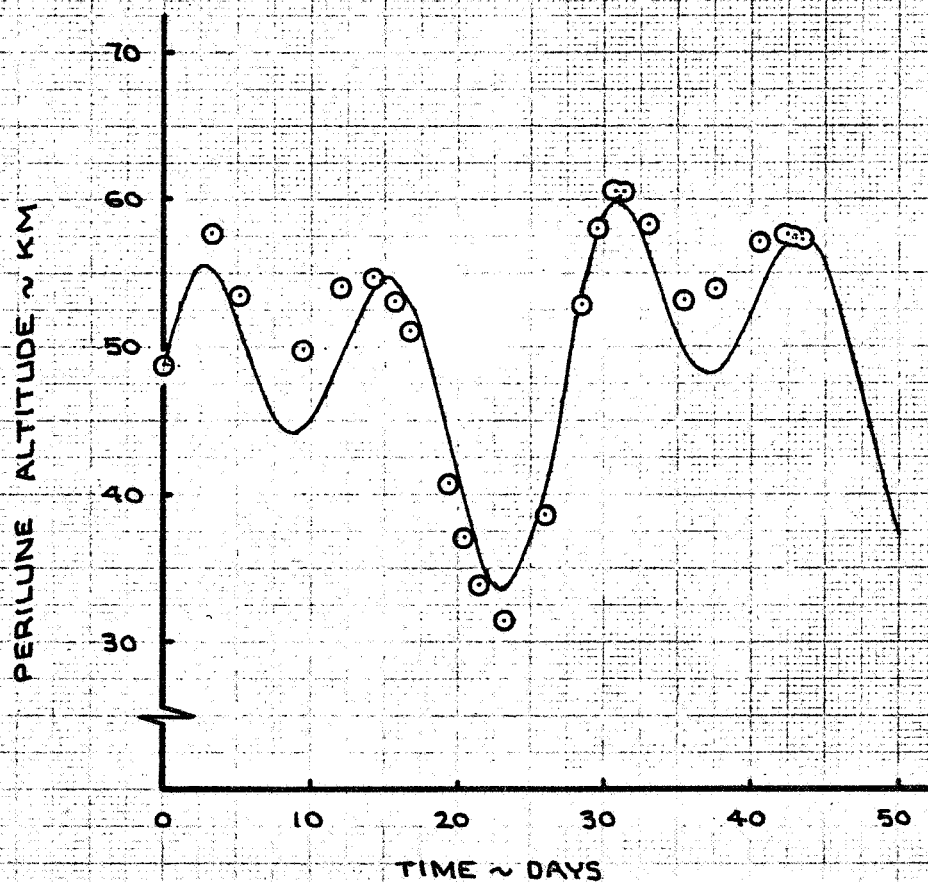


FIGURE 6-17

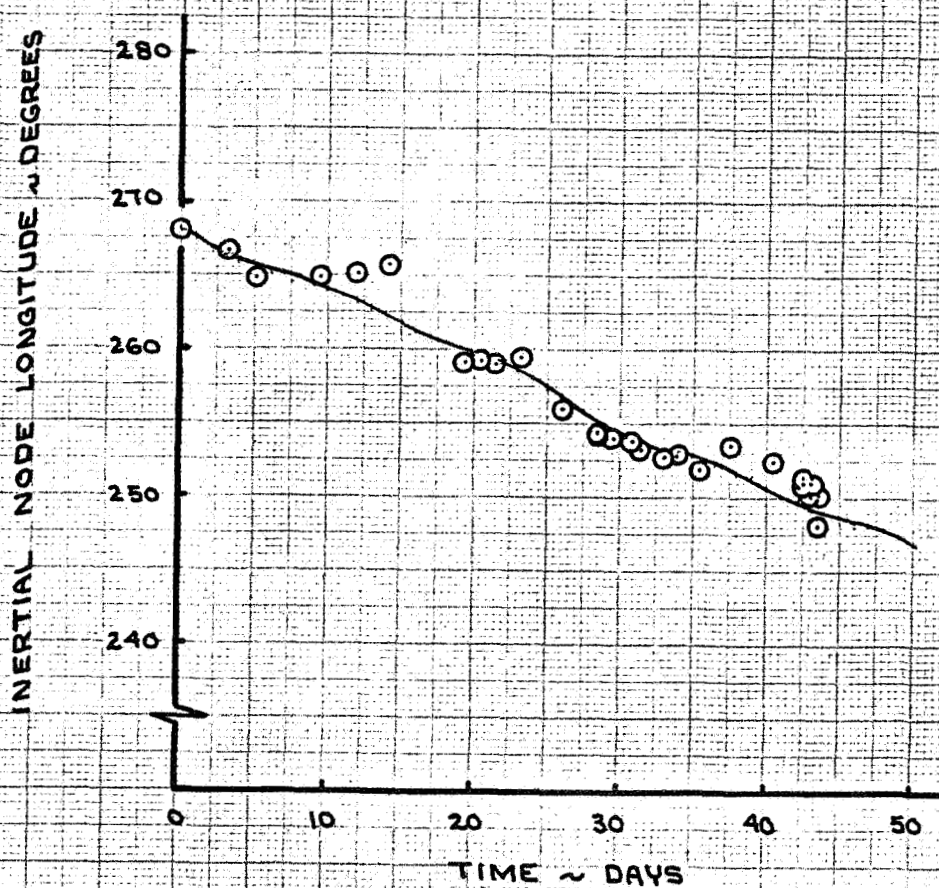
NODE LONGITUDE HISTORY
LUNAR ORBITER I - PHASE 7INITIAL CONDITIONS : 00 7000-4
O O0 SOLUTIONS
— MODEL R-2

FIGURE 6-18

ARGUMENT OF PERILUNE HISTORY
LUNAR ORBITER I - PHASE 7

INITIAL CONDITIONS : OD 7000-4

○ OD SOLUTION

— MODEL R-2

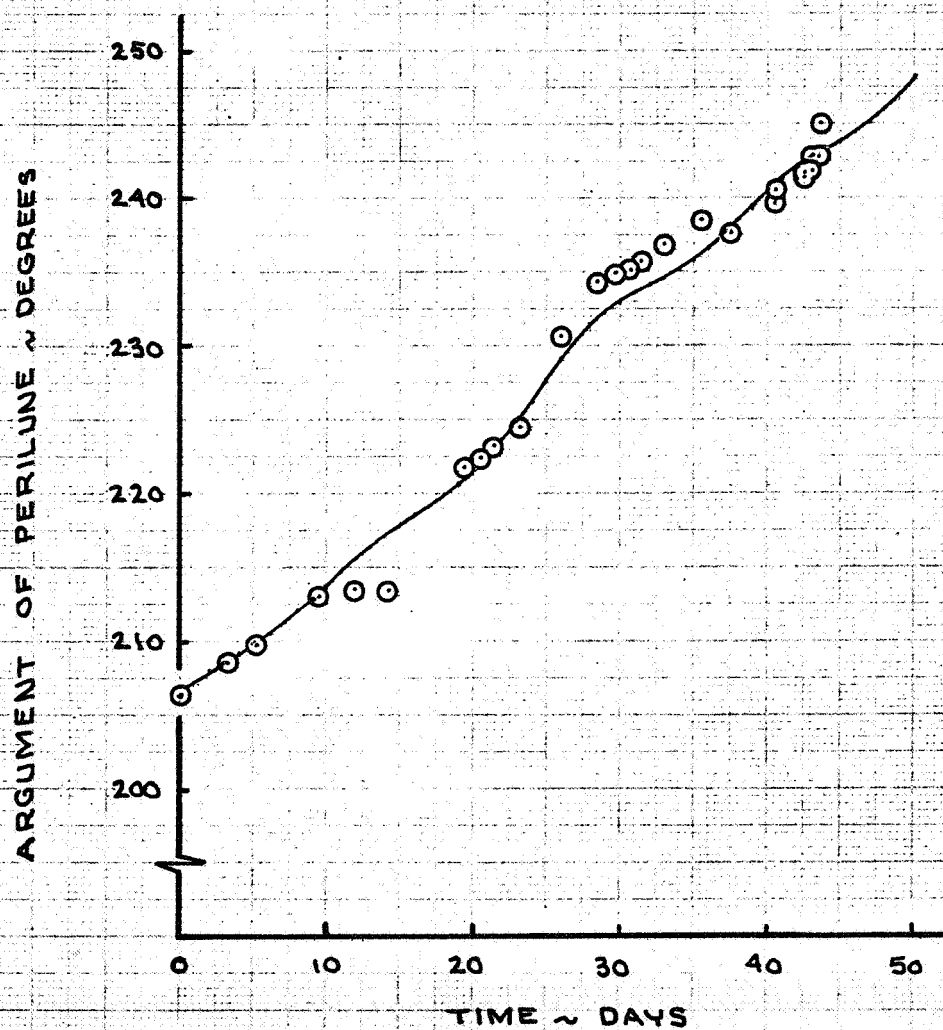


FIGURE 6-19

ORBIT INCLINATION HISTORY LUNAR ORBITER I - PHASE 7

INITIAL CONDITIONS: 00 7000-4
O O O SOLUTIONS

— MODEL R-2

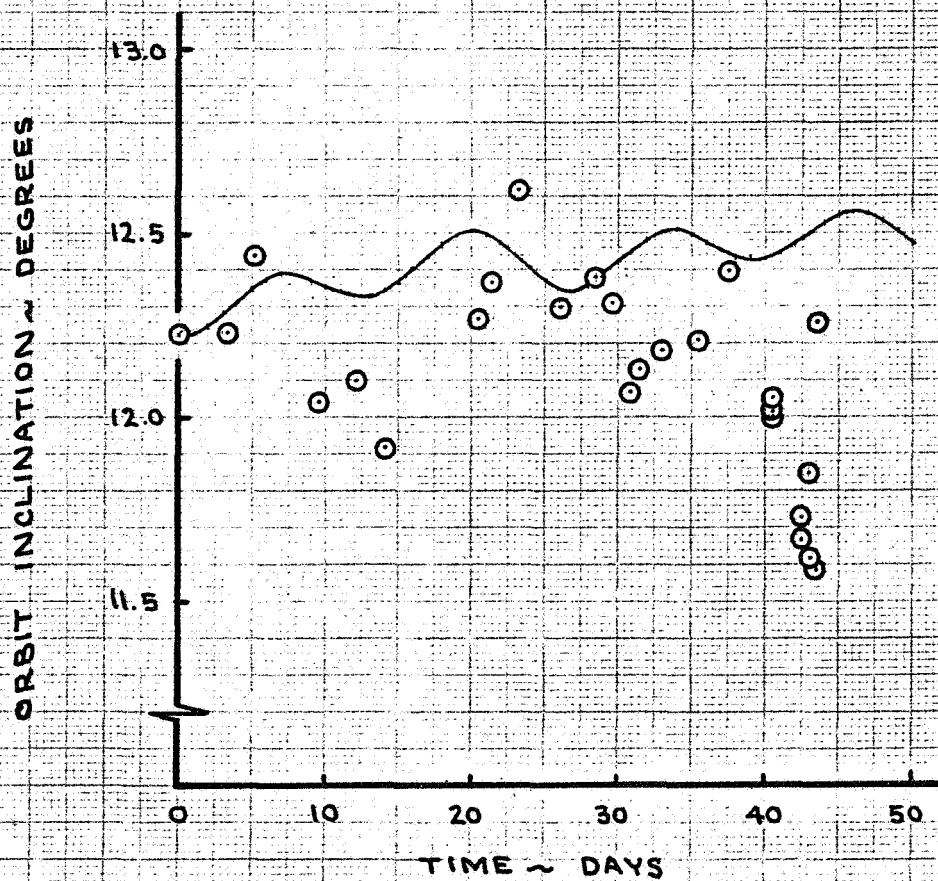


FIGURE 6-20

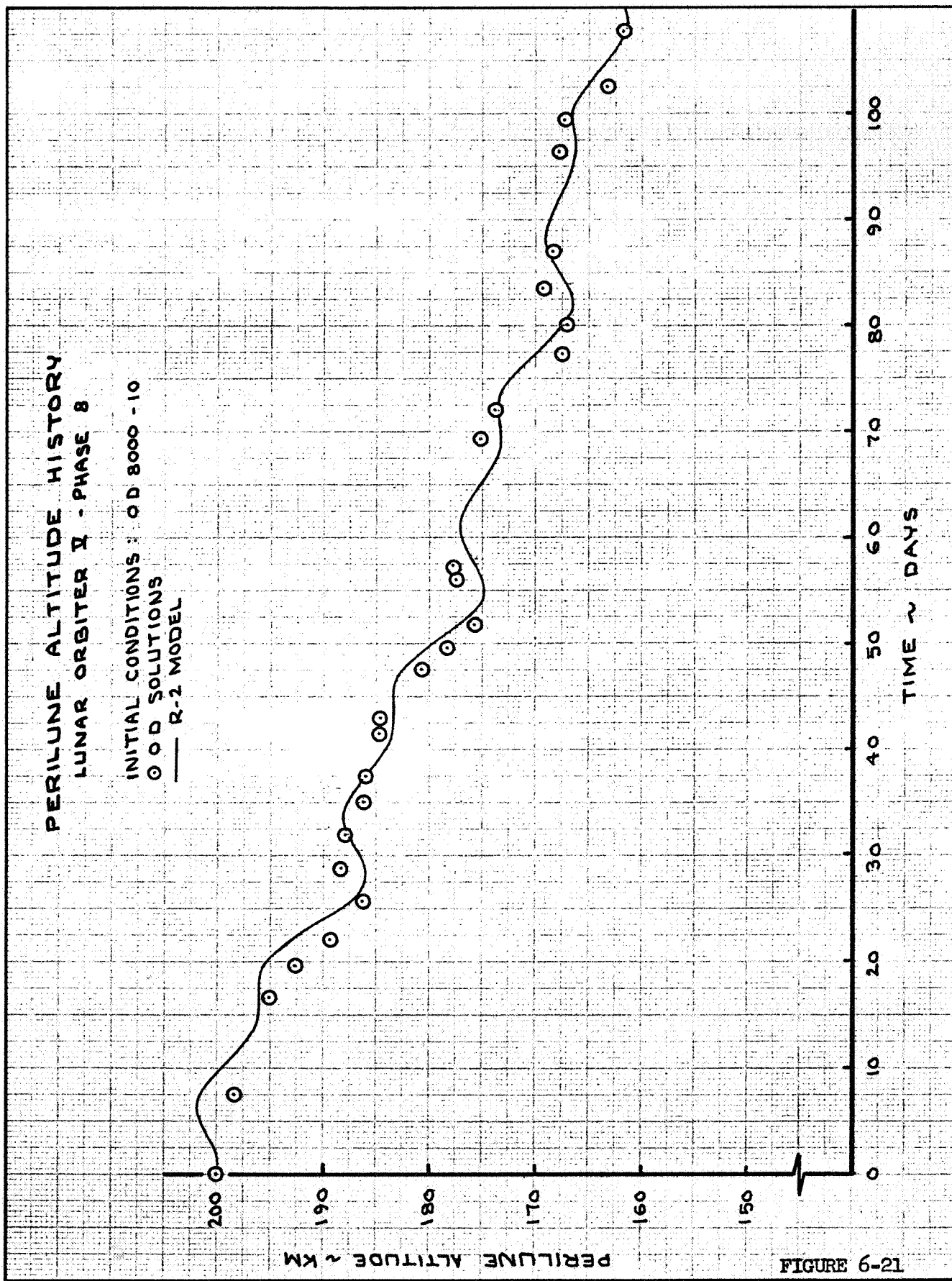


FIGURE 6-21

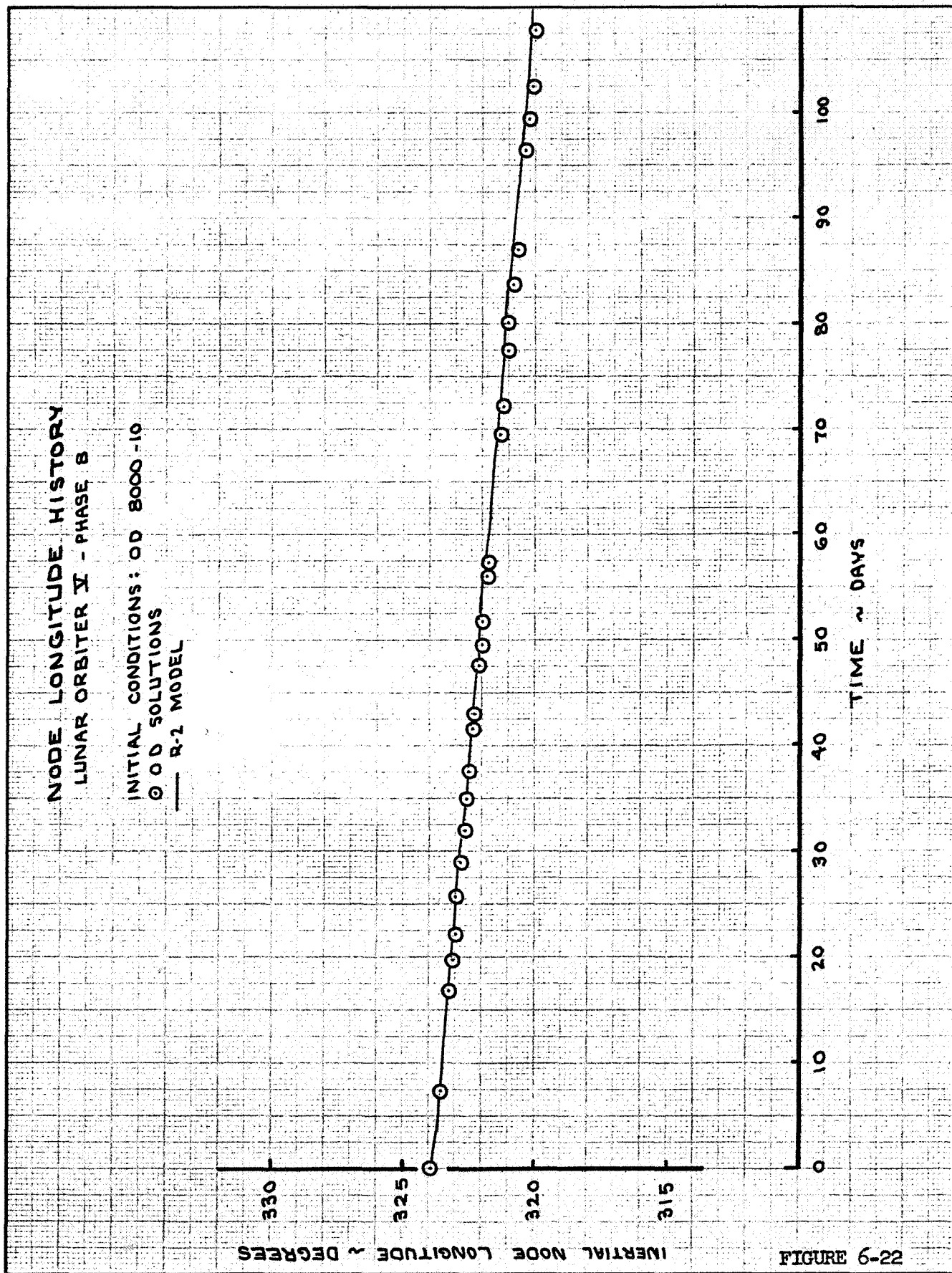
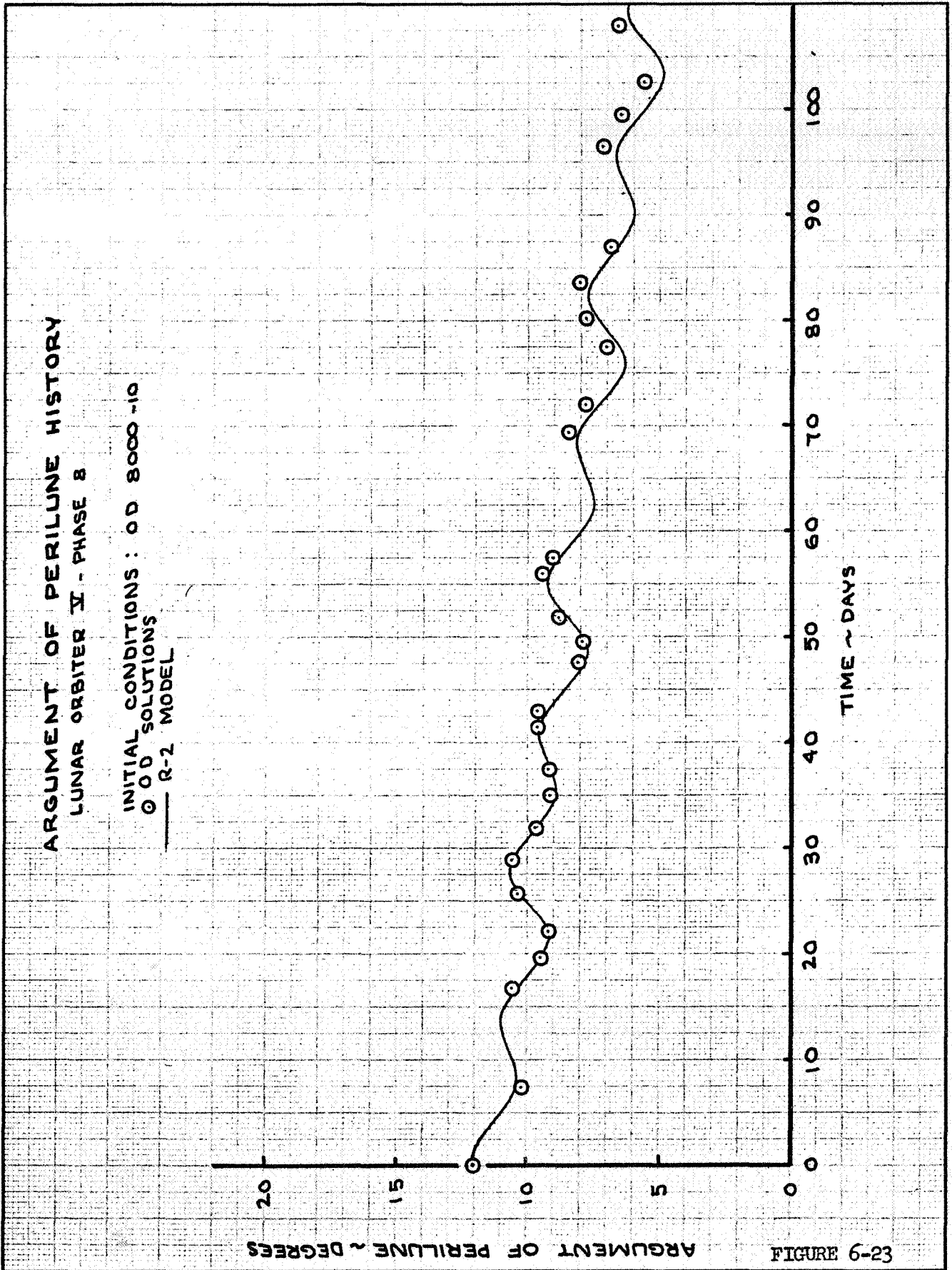


FIGURE 6-22



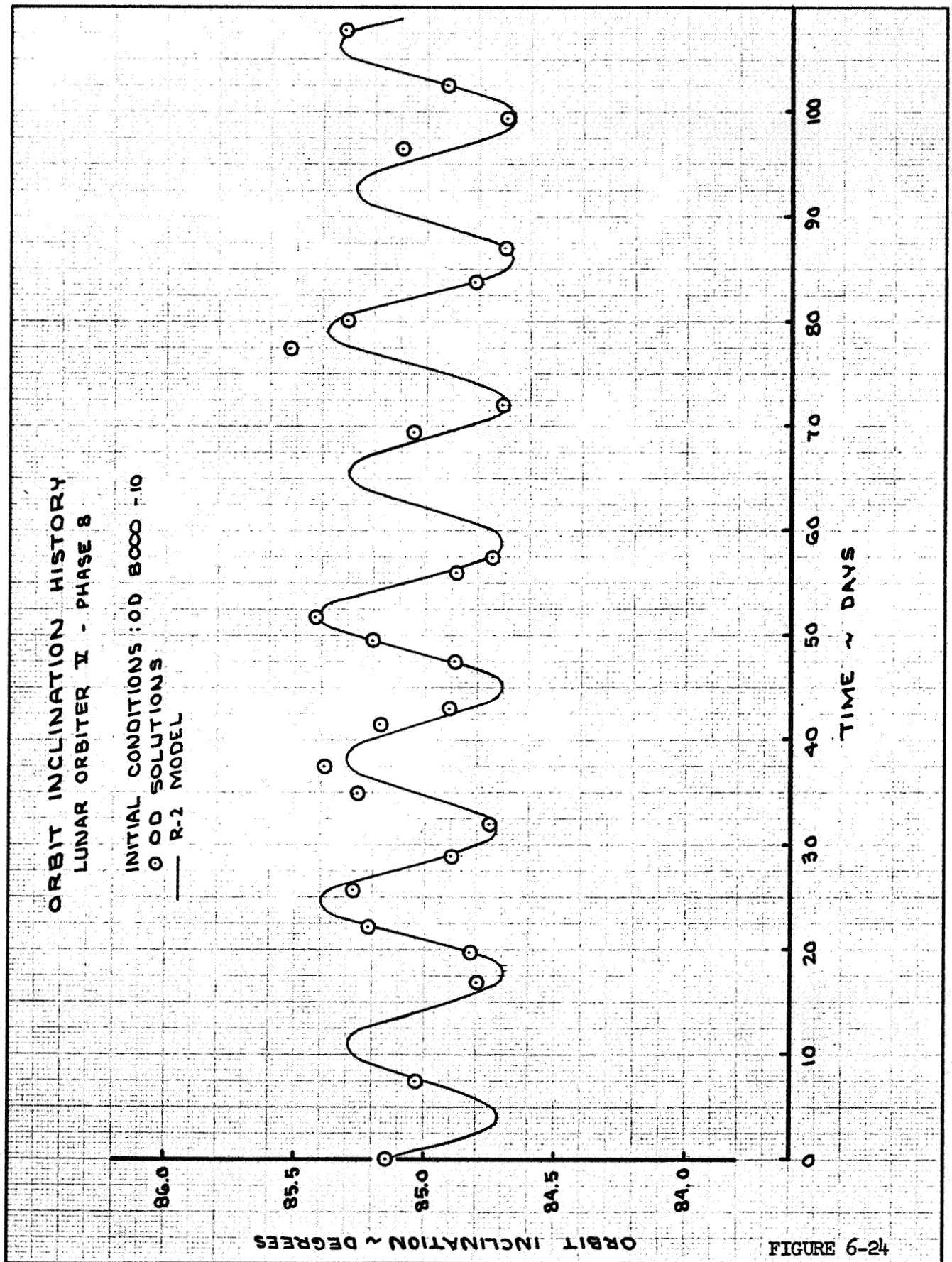


FIGURE 6-24

7.0 APOLLO ORBIT PERTURBATIONS

Orbit element histories have been calculated for the Apollo orbit (both the elliptical and circular orbits) using the R-2 model and are presented in Figures 7-1 through 7-4. For comparison, the histories are also shown for the triaxial moon model. Initial conditions are as follows:

Date	December 24, 1963
Apolune altitude	170 n. mi.
Perilune altitude	60 n. mi.
Selenographic node longitude	52 degrees
Argument of perilune	180 degrees
Inclination	168 degrees

After two complete revolutions in the elliptical orbit (4.3 hours), apolune altitude is lowered to 60 nautical miles; no other orbit adjustments are made.

It is noted that with the R-2 model, perilune in the initial elliptical orbit increases from 60 to 60.35 n. mi. by the time of orbit transfer. This point on the orbit now becomes apolune, and the new perilune moves to a location of approximately -44° and decreases by approximately 2 n. mi. after 8 revolutions (21.14 hours after lunar orbit insertion).

If it is assumed that accurate orbit determinations are made each orbit and that the state will be forwarded no more than 3 hours for the trans-earth injection maneuver, an error of approximately 0.4 nautical miles may be encountered by using the triaxial moon model to forward the state.

USE FOR TYPEWRITTEN MATERIAL ONLY

PERILUNE ALTITUDE PREDICTION APOLLO MISSION

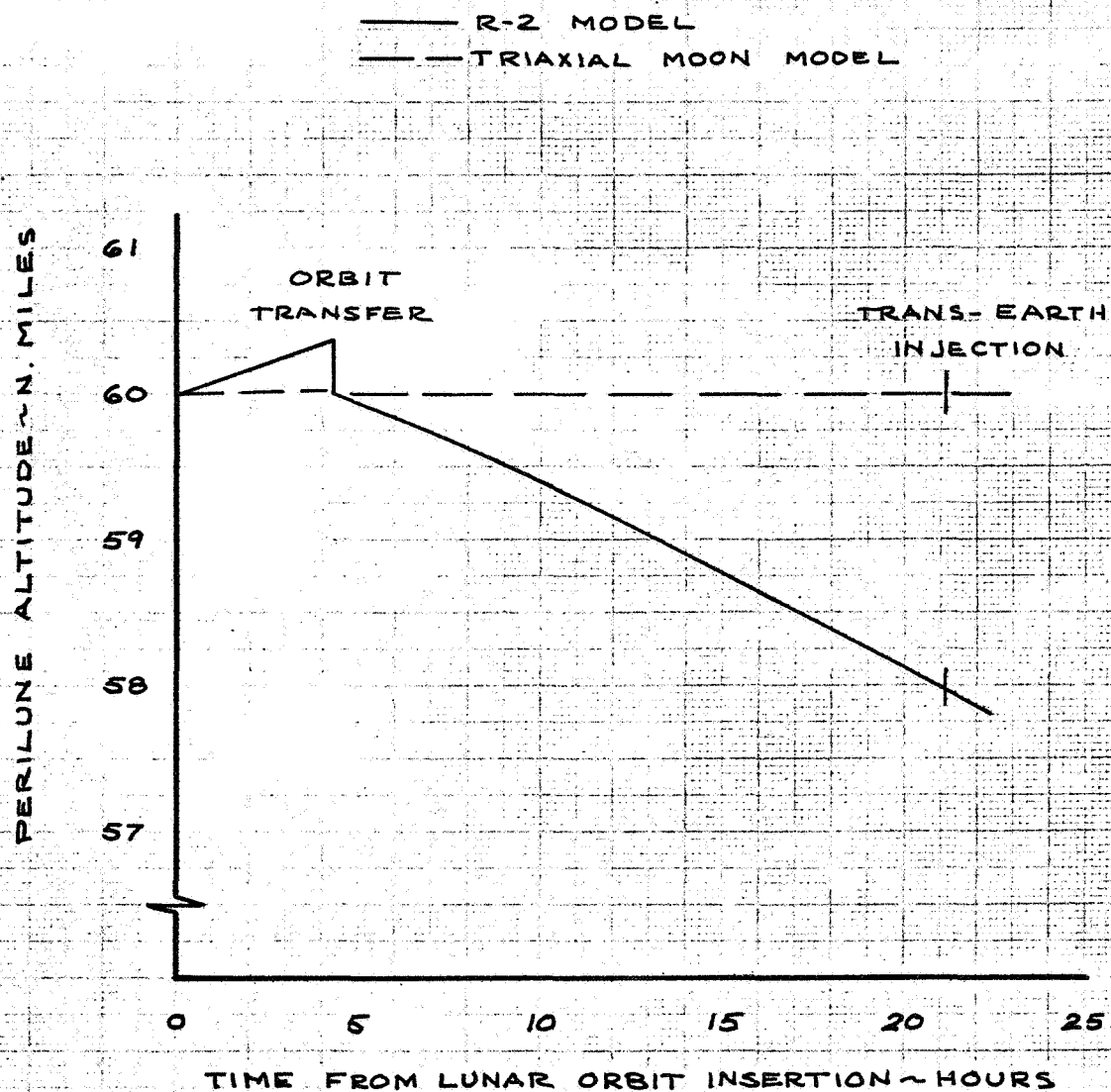


FIGURE 7-1

NODE LONGITUDE PREDICTION APOLLO MISSION

R-2 OR TRIAXIAL MOON MODEL

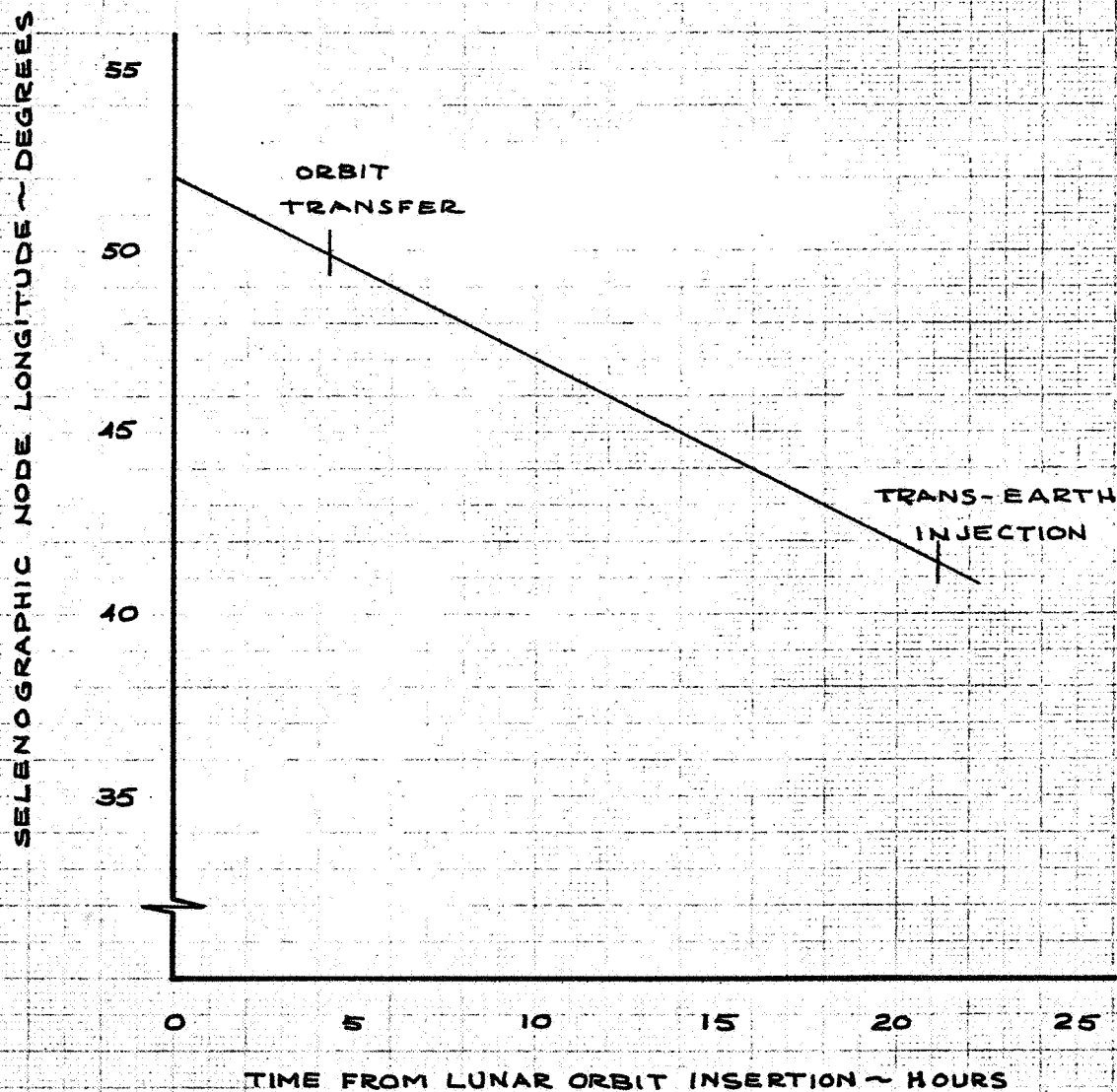


FIGURE 7-2

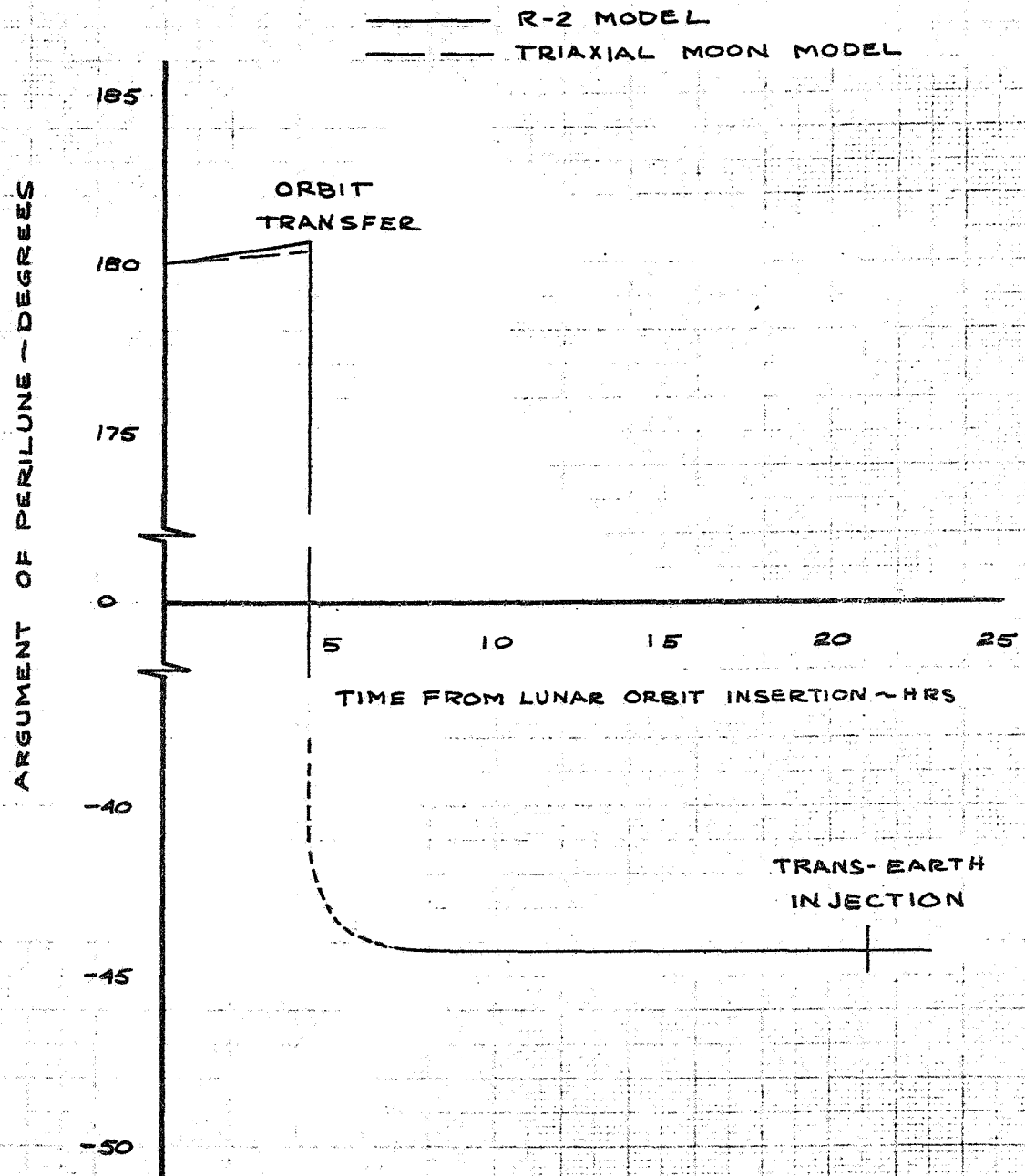
ARGUMENT OF PERILUNE PREDICTION
APOLLO MISSION

FIGURE 7-3

ORBIT INCLINATION PREDICTION APOLLO MISSION

R-2 OR TRIAXIAL MOON MODEL

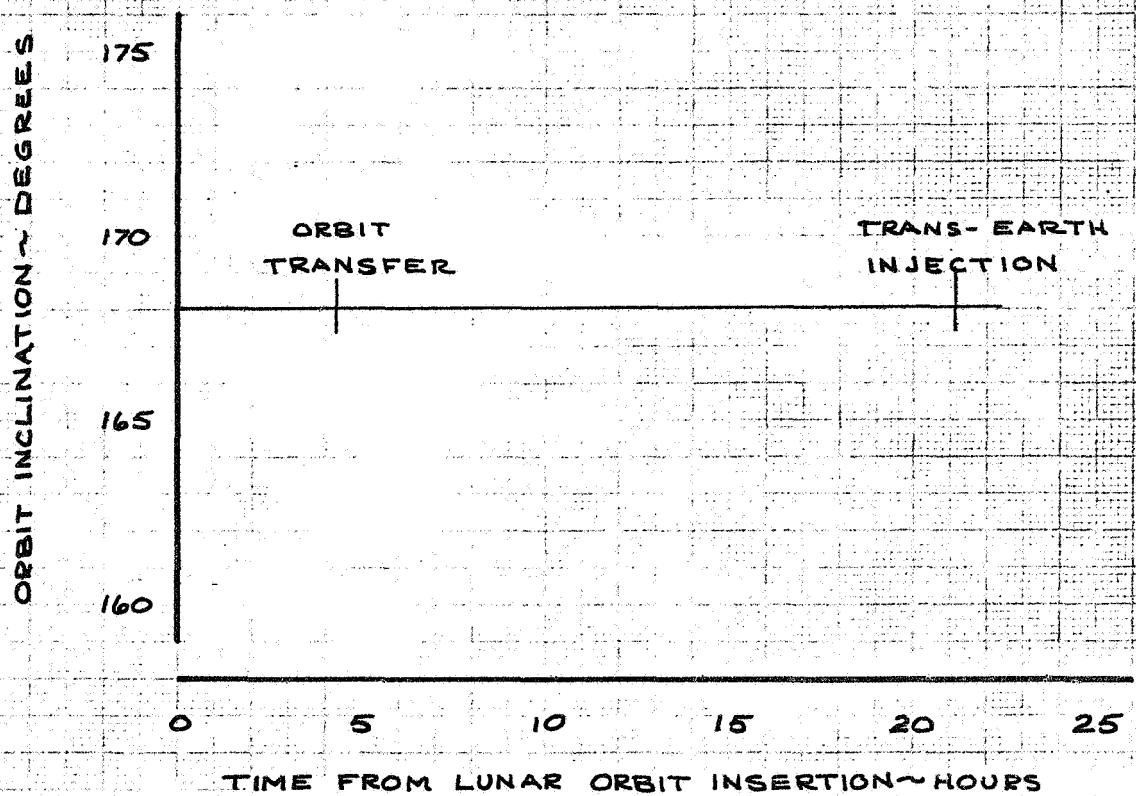


FIGURE 7-4

8.0 CONCLUSIONS AND RECOMMENDATIONS

A simple 4-coefficient lunar gravitational model has been developed using tracking data from Lunar Orbiter missions. It has been shown that the model accurately predicts orbit element histories for a range of initial conditions (inclinations of 12° , 21° and 85° , and eccentricities of 0.04 to 0.3). It is recommended that this model be used for Apollo mission control and for lunar mission design work requiring long term orbit predictions.

It is further recommended that additional analyses be performed to improve this model. It is believed that the addition of one more coefficient (S_{31}) will produce a small phase shift in the perturbations which are dependent on selenographic longitude and therefore will improve the predictions in perilune altitude and argument of perilune.

USE FOR TYPEWRITTEN MATERIAL ONLY

9.0 REFERENCES

1. Barrow, G. D., "Evaluation of Nine Lunar Models for Apollo - Final Report," Document D2-100820-1, December 1968, The Boeing Company, Seattle, Washington.
2. Gapcynski, John P., "The Lunar Gravitational Field as Determined from the Tracking Data of the Lunar Orbiter Series of Spacecraft," ASS Paper 68-132, September 1968.
3. Mueller, Ivan I., "Introduction to Satellite Geodesy," Frederick Ungar Publishing Company, 1964.

USE FOR TYPEWRITTEN MATERIAL ONLY

APPENDIX

The lunar gravitational potential function is defined by the following expression:

$$U = \frac{GM_M}{r} \left[1 + \sum_{n=2}^{\infty} \sum_{m=0}^n \left(\frac{R_M}{r} \right)^n P_{nm}(\sin \phi) (C_{nm} \cos m \lambda + S_{nm} \sin m \lambda) \right]$$

Orbit element perturbation equations may be derived from this expression and with the inclusion of third body (earth) effects. Third body effects are taken from Reference 2 with the assumption that the sub-earth point is at a selenographic position of 0 latitude and 0 longitude. The perturbation equations are defined below with the definition of nomenclature immediately following. Note that by convention, when $m = 0$, $C_{no} = -J_{no}$. These equations are limited to the coefficients J_{20} , J_{30} , J_{40} , C_{22} , and C_{31} .

$$\dot{a} = 0$$

$$\dot{e} = \dot{e}_{30} + \dot{e}_{31} + \dot{e}_{40} + \dot{e}_E$$

$$\dot{e}_{30} = \frac{3n}{2} \frac{R_M^3}{a^3(1-e^2)^2} J_{30} \sin i \left(\frac{5}{4} \sin^2 i - 1 \right) \cos \omega$$

$$\begin{aligned} \dot{e}_{31} = \frac{3n}{8} \frac{R_M^3}{a^3(1-e^2)^2} C_{31} & \left[(5 \sin^2 i - 4) \sin \omega \cos \Omega_s \right. \\ & \left. + (15 \sin^2 i \cos i - 4 \cos i) \cos \omega \sin \Omega_s \right] \end{aligned}$$

$$\dot{e}_{40} = -\frac{15n}{32} \frac{R_M^4}{a^4(1-e^2)^3} J_{40} \sin^2 i (6 - 7 \sin^2 i) \sin 2 \omega$$

$$\begin{aligned} \dot{e}_E = \frac{15}{4n} \frac{GM_E}{R_{EM}^3} e (1-e^2)^{1/2} & \left[\sin 2 \Omega_s \cos 2 \omega \cos i \right. \\ & \left. + (\cos^2 \Omega_s - \sin^2 \Omega_s \cos^2 i) \sin 2 \omega \right] \end{aligned}$$

$$\left(\frac{di}{dt} \right) = \left(\frac{di}{dt} \right)_{22} + \left(\frac{di}{dt} \right)_{30} + \left(\frac{di}{dt} \right)_{31} + \left(\frac{di}{dt} \right)_{40} + \left(\frac{di}{dt} \right)_E$$

$$\left(\frac{di}{dt} \right)_{22} = 3n \frac{R_M^2}{a^2(1-e^2)^2} C_{22} \sin i \sin 2 \Omega_s$$

USE FOR TYPEWRITTEN MATERIAL ONLY

APPENDIX (Continued)

$$\left(\frac{di}{dt}\right)_{30} = -\frac{3n}{2} \frac{R_M^3 e}{a^3(1-e^2)^3} J_{30} \cos i \left(\frac{5}{4} \sin^2 i - 1\right) \cos \omega$$

$$\left(\frac{di}{dt}\right)_{31} = \frac{3n}{8} \frac{R_M^3 e}{a^3(1-e^2)^3} C_{31} \sin i \left[10 \cos i \sin \omega \cos \Omega_s + (1-15 \cos^2 i) \cos \omega \sin \Omega_s \right]$$

$$\left(\frac{di}{dt}\right)_{40} = \frac{15n}{32} \frac{R_M^4 e^2}{a^4(1-e^2)^4} J_{40} \sin i \cos i (6-7 \sin^2 i) \sin 2 \omega$$

$$\left(\frac{di}{dt}\right)_E = \frac{3}{4n} \frac{GM_E}{R_{EM}^2} \frac{\sin \Omega_s \sin i}{(1-e^2)^{1/2}} \left[\cos \Omega_s (2+3e^2+5e^2 \cos 2 \omega) - 5 e^2 \sin \Omega_s \sin 2 \omega \cos i \right]$$

$$\dot{\omega} = \dot{\omega}_{20} + \dot{\omega}_{22} + \dot{\omega}_{30} + \dot{\omega}_{31} + \dot{\omega}_{40} + \dot{\omega}_E$$

$$\dot{\omega}_{20} = \frac{3n}{4} \frac{R_M^2}{a^2(1-e^2)^2} J_{20} (4-5 \sin^2 i)$$

$$\dot{\omega}_{22} = \frac{3n}{2} \frac{R_M^2}{a^2(1-e^2)^2} C_{22} \cos 2 \Omega_s (5 \sin^2 i - 2)$$

$$\dot{\omega}_{30} = -\frac{3n}{2} \frac{R_M^3}{a^3(1-e^2)^3} J_{30} \sin \omega \left[\left(\frac{1+4e^2}{e} \right) \sin i \left(\frac{5}{4} \sin^2 i - 1 \right) - e \frac{\cos^2 i}{\sin i} \left(\frac{15}{4} \sin^2 i - 1 \right) \right]$$

$$\dot{\omega}_{31} = \frac{-3n}{64} \frac{R_M^3 (1+4e^2)}{a^3 e (1-e^2)^3} C_{31} \left[(12+20 \cos 2 i) \cos \omega \cos \Omega_s - (2 \cos i + 30 \cos 3 i) \sin \omega \sin \Omega_s \right] - \dot{\Omega}_{I31} \cos i$$

$$\begin{aligned} \dot{\omega}_{40} = & \frac{-15n}{32} \frac{R_M^4}{a^4(1-e^2)^4} J_{40} \left[(16-62 \sin^2 i + 49 \sin^4 i) \right. \\ & + \frac{9}{4} e^2 (8-28 \sin^2 i + 21 \sin^4 i) \\ & + (6-7 \sin^2 i) \sin^2 i \cos 2 \omega \\ & \left. - \frac{e^2}{2} (12-70 \sin^2 i + 63 \sin^4 i) \cos 2 \omega \right] \end{aligned}$$

USE FOR TYPEWRITTEN MATERIAL ONLY

APPENDIX (Continued)

$$\begin{aligned} \dot{\omega}_E = & \frac{3}{2n} \frac{GM_E}{R_{EM}^3} (1-e^2)^{1/2} \left\{ -\frac{5}{2} \sin 2 \Omega_s \cos i \sin 2 \omega \right. \\ & + \frac{5}{2} (\cos^2 \Omega_s - \sin^2 \Omega_s \cos^2 i) \cos 2 \omega \\ & - 1 + \frac{3}{2} (\cos^2 \Omega_s + \sin^2 \Omega_s \cos^2 i) \\ & + \frac{5 a}{2 R_{EM} e (1-e^2)^{1/2}} (\cos \Omega_s \cos \omega - \sin \Omega_s \cos i \sin \omega) \\ & \left. \left[1 - \frac{5}{4} (\cos^2 \Omega_s + \sin^2 \Omega_s \cos^2 i) \right] \right\} - \Omega_{I_E} \cos i \end{aligned}$$

$$\dot{\Omega}_I = \dot{\Omega}_{I_{20}} + \dot{\Omega}_{I_{22}} + \dot{\Omega}_{I_{30}} + \dot{\Omega}_{I_{31}} + \dot{\Omega}_{I_{40}} + \dot{\Omega}_{I_E}$$

$$\dot{\Omega}_{I_{20}} = -\frac{3n}{2} \frac{R_M^2}{a^2(1-e^2)^2} J_{20} \cos i$$

$$\dot{\Omega}_{I_{22}} = \frac{3n R_M^2}{a^2(1-e^2)^2} C_{22} \cos i \cos 2 \Omega_s$$

$$\dot{\Omega}_{I_{30}} = \frac{-3n R_M^3}{2 a^3(1-e^2)^3} e J_{30} \cot i \left(\frac{15}{4} \sin^2 i - 1 \right) \sin \omega$$

$$\begin{aligned} \dot{\Omega}_{I_{31}} = & \frac{-3n}{16} \frac{R_M^3}{a^3(1-e^2)^3} e C_{31} \left[-20 \cos i \cos \omega \cos \Omega_s \right. \\ & \left. - (22-90 \cos^2 i) \sin \omega \sin \Omega_s \right] \end{aligned}$$

$$\begin{aligned} \dot{\Omega}_{I_{40}} = & \frac{15 n}{16} \frac{R^4}{a^4(1-e^2)^4} J_{40} \cos i \left[\left(1 + \frac{3}{2} e^2 \right) (4-7 \sin^2 i) \right. \\ & \left. - e^2 (3-7 \sin^2 i) \cos 2 \omega \right] \end{aligned}$$

$$\begin{aligned} \dot{\Omega}_{I_E} = & \frac{3}{4n} \frac{GM_E \sin \Omega_s}{R_{EM}^3 (1-e^2)^{1/2}} \left[5 e^2 \cos \Omega_s \sin 2 \omega \right. \\ & \left. - \sin \Omega_s \cos i (2 + 3 e^2 - 5 e^2 \cos 2 \omega) \right] \end{aligned}$$

USE FOR TYPEWRITTEN MATERIAL ONLY

APPENDIX (Continued)

Nomenclature

a	semi-major axis of the orbit
e	eccentricity of the orbit
i	inclination of the orbit
n	mean motion, $\frac{(GM)^{1/2}}{a^{3/2}}$
r	selenocentric radius of the spacecraft
C_{nm}	harmonic coefficient
GM_M	gravitational constant of the moon, $4902.5801 \text{ km}^3/\text{sec}^2$
GM_E	gravitational constant of the earth, $398601.28 \text{ km}^3/\text{sec}^2$
$J_{no} = -C_{no}$	harmonic coefficient
P_{nm}	associated Legendre polynomials
R_M	moon radius, 1738.09 km
R_{EM}	earth-moon radius, function of date
S_{nm}	harmonic coefficient
ϕ	selenographic latitude of spacecraft
λ	selenographic longitude of spacecraft
ω	argument of perilune of the orbit
Ω_I	inertial node longitude of the orbit, referenced to the prime meridian at epoch
Ω_S	selenographic node longitude of the orbit

Subscripts

20	}	relating to the particular harmonic coefficient
22		
30		
31		
40		
E		relating to the earth

USE FOR TYPEWRITTEN MATERIAL ONLY

LIMITATIONS

DDC DOES NOT APPLY

This document is controlled by organization 2-7837.

All revisions to this document shall be approved by the
above noted organization prior to release.

ACTIVE SHEET RECORD

SHEET NO.	REV LTR	ADDED SHEETS				SHEET NO.	REV LTR	ADDED SHEETS			
		SHEET NO.	REV LTR	SHEET NO.	REV LTR			SHEET NO.	REV LTR	SHEET NO.	REV LTR
1						41					
11						42					
111						43					
iv						44					
						45					
1						46					
2						47					
3						48					
4						49					
5						50					
6						51					
7						52					
8						53					
9						54					
10						55					
11						56					
12						57					
13						58					
14						59					
15											
16											
17											
18											
19											
20											
21											
22											
23											
24											
25											
26											
27											
28											
29											
30											
31											
32											
33											
34											
35											
36											
37											
38											
39											
40											

REV LTR _____

BOEING

NO. D2-100819-1